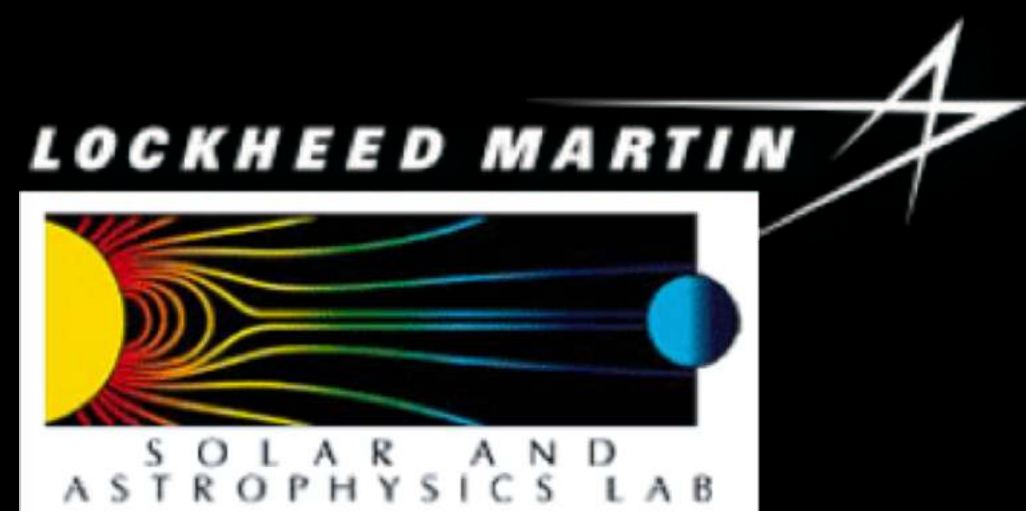




Study Solar Eruptions from a Global Perspective: Current Status and Future Improvements on the Global MHD Models

Meng Jin

Lockheed Martin Solar and Astrophysics Lab (LMSAL), Palo Alto, CA, USA



RoCS/MUSE/IRIS Workshop, Feb 27-Mar 2, Svalbard, Norway



Global MHD Modeling of Solar Atmosphere and Solar Wind

- The global MHD models of solar atmosphere solve **ideal MHD equations** with different treatments of **coronal heating term**:
 - **Variable polytropic index** (e.g., Usmanov 1993, Linker et al. 1999, Mikic et al. 1999, Roussev et al. 2003, Riley et al. 2006; Cohen et al. 2007).
 - **Geometric heating or cooling functions** (e.g., Lionello et al. 2009; Downs et al. 2010).
 - **Heating by Alfvén-waves** (e.g., Usmanov et al. 2000, Usmanov & Goldstein 2003, Evans et al. 2012).
- In addition to MHD equations, wave-driven models need to solve **wave kinetic equation** that describe the exchange of momentum and energy between the plasma and the wave field (e.g., Suzuki & Inutsuka 2005, Cranmer et al. 2009, Lionello et al. 2014, Réville et al. 2020).
- The main challenges for global wave-driven models:
 - Taking into account different wave behaviors within the inhomogeneous plasma environment (e.g., **wave reflection, wave dissipation**).
 - Unifying the treatment of wave dissipation in different **magnetic topologies** (i.e., open and closed field lines).

Alfvén Wave Solar Model (AWS \odot M)

$$\frac{\partial \rho}{\partial t} + \nabla \cdot (\rho \mathbf{u}) = 0 \quad (1)$$

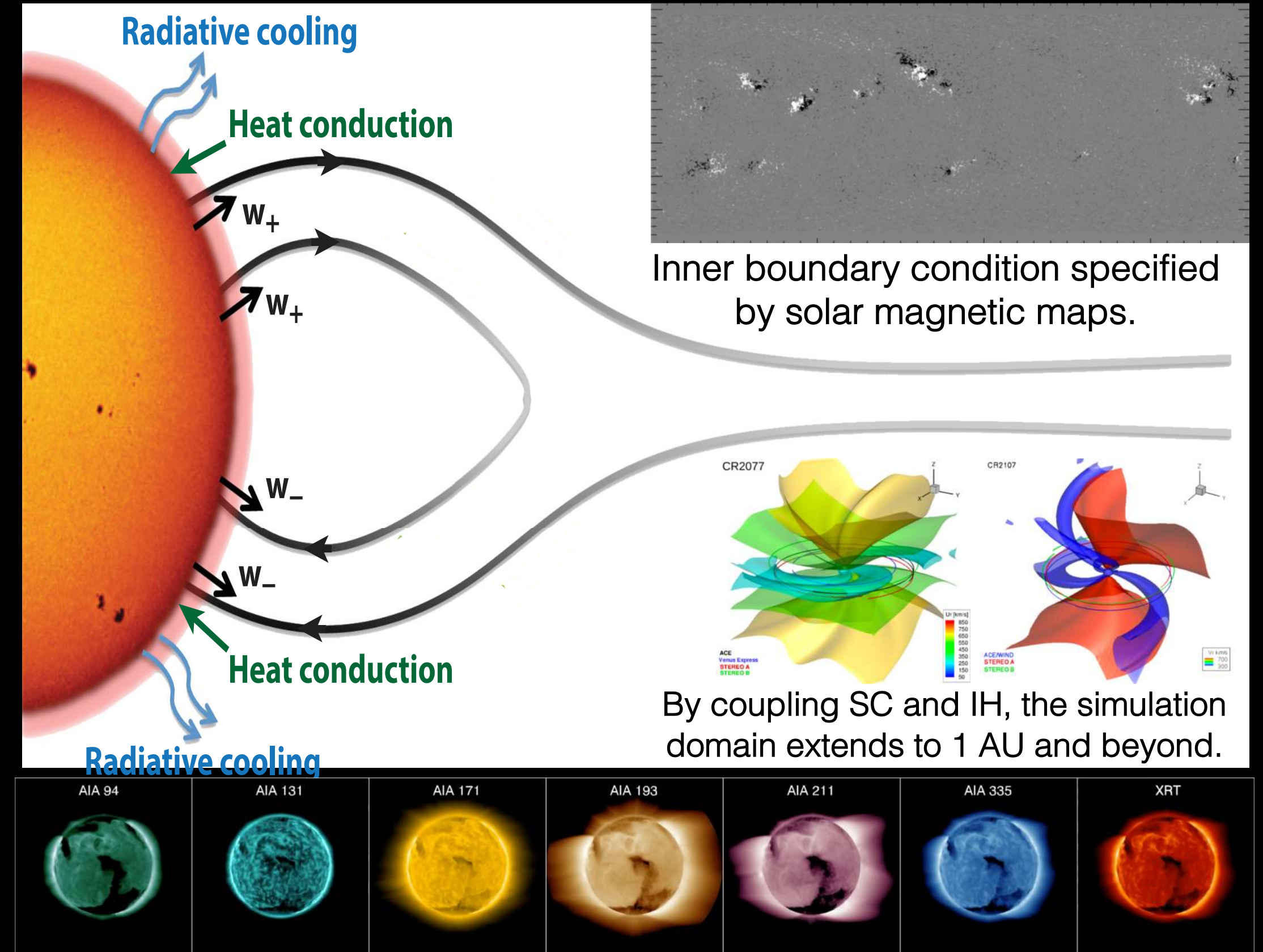
$$\frac{\partial(\rho \mathbf{u})}{\partial t} + \nabla \cdot \left(\rho \mathbf{u} \mathbf{u} - \frac{\mathbf{B} \mathbf{B}}{4\pi} \right) + \nabla \left(p_p + p_e + \frac{w_+ + w_-}{2} + \frac{B^2}{8\pi} \right) = -\rho \frac{GM_\odot}{r^2} \mathbf{e}_r \quad (2)$$

$$\frac{\partial \left(\frac{p_e}{\gamma-1} \right)}{\partial t} + \nabla \cdot \left(\frac{p_e}{\gamma-1} \mathbf{u} \right) = -p_e \nabla \cdot \mathbf{u} + \frac{2}{\tau_{pe}} (p_p - p_e) - \nabla \cdot \mathbf{q}_e - Q_{\text{rad}} + \alpha Q_w \quad (3)$$

$$\frac{\partial \left(\frac{p_p}{\gamma-1} \right)}{\partial t} + \nabla \cdot \left(\frac{p_p}{\gamma-1} \mathbf{u} \right) = -p_p \nabla \cdot \mathbf{u} + \frac{2}{\tau_{pe}} (p_e - p_p) + (1 - \alpha) Q_w \quad (4)$$

$$\frac{\partial w_\pm}{\partial t} + \nabla \cdot [w_\pm (\mathbf{u} \pm \mathbf{u}_A)] = -\frac{w_\pm}{2} \nabla \cdot \mathbf{u} - \Gamma_\pm w_\pm \quad (5)$$

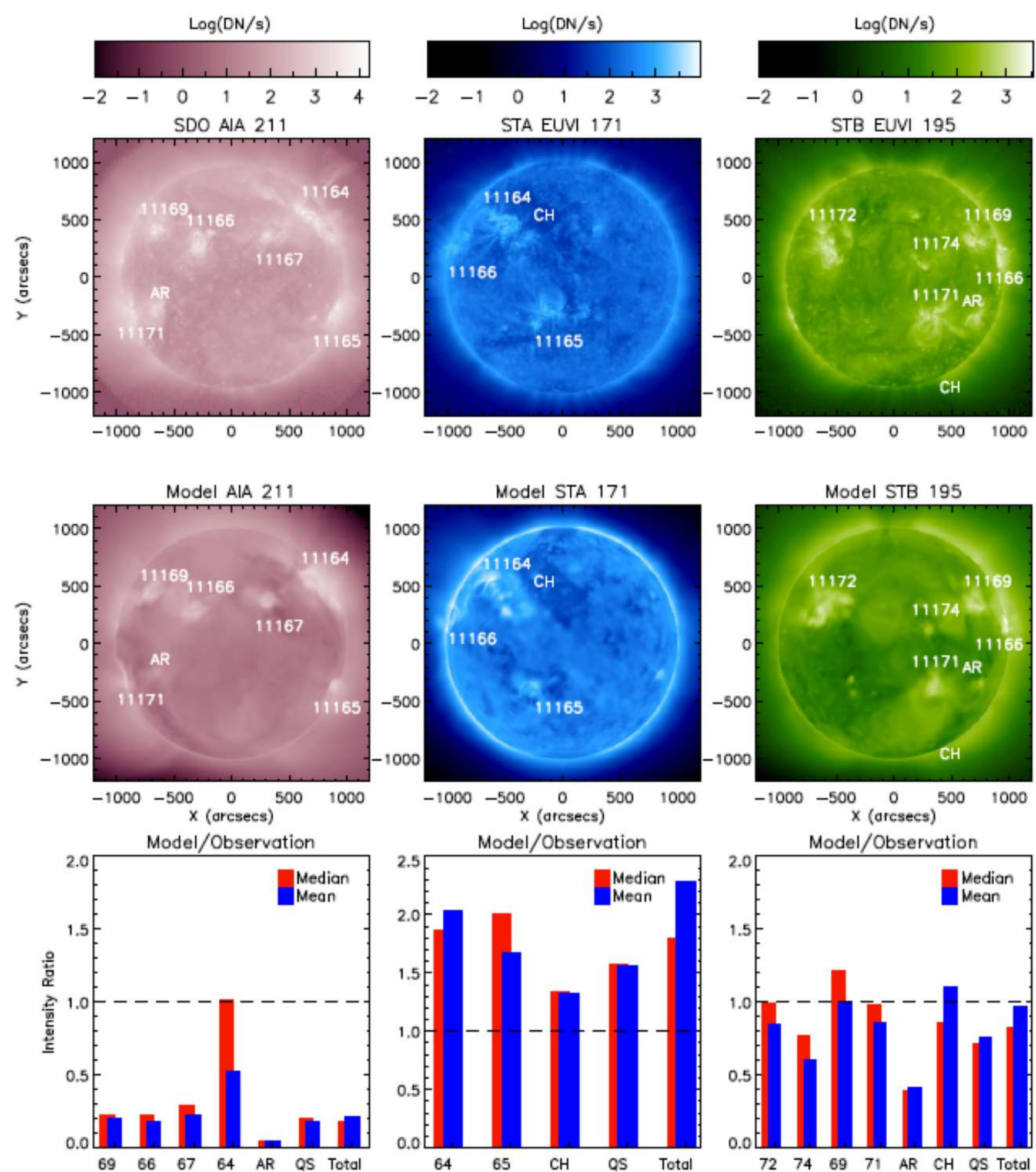
$$\frac{\partial \mathbf{B}}{\partial t} - \nabla \times (\mathbf{u} \times \mathbf{B}) = 0 \quad (6)$$



- **Alfvén Wave Solar Model** (van der Holst et al. 2014), developed within Space Weather Modeling Framework (SWMF; Toth et al. 2012) at U of Michigan.
- **Coronal heating and solar wind accelerating by Alfvén waves.** Physically consistent treatment of wave reflection, dissipation, and heat partitioning between the **electrons** and **protons**.
- Model starts from upper chromosphere including **heat conduction** (both collisional and collisionless) and **radiative cooling**.
- Adaptive mesh refinement (**AMR**) to resolve structures (e.g., current sheets, shocks).

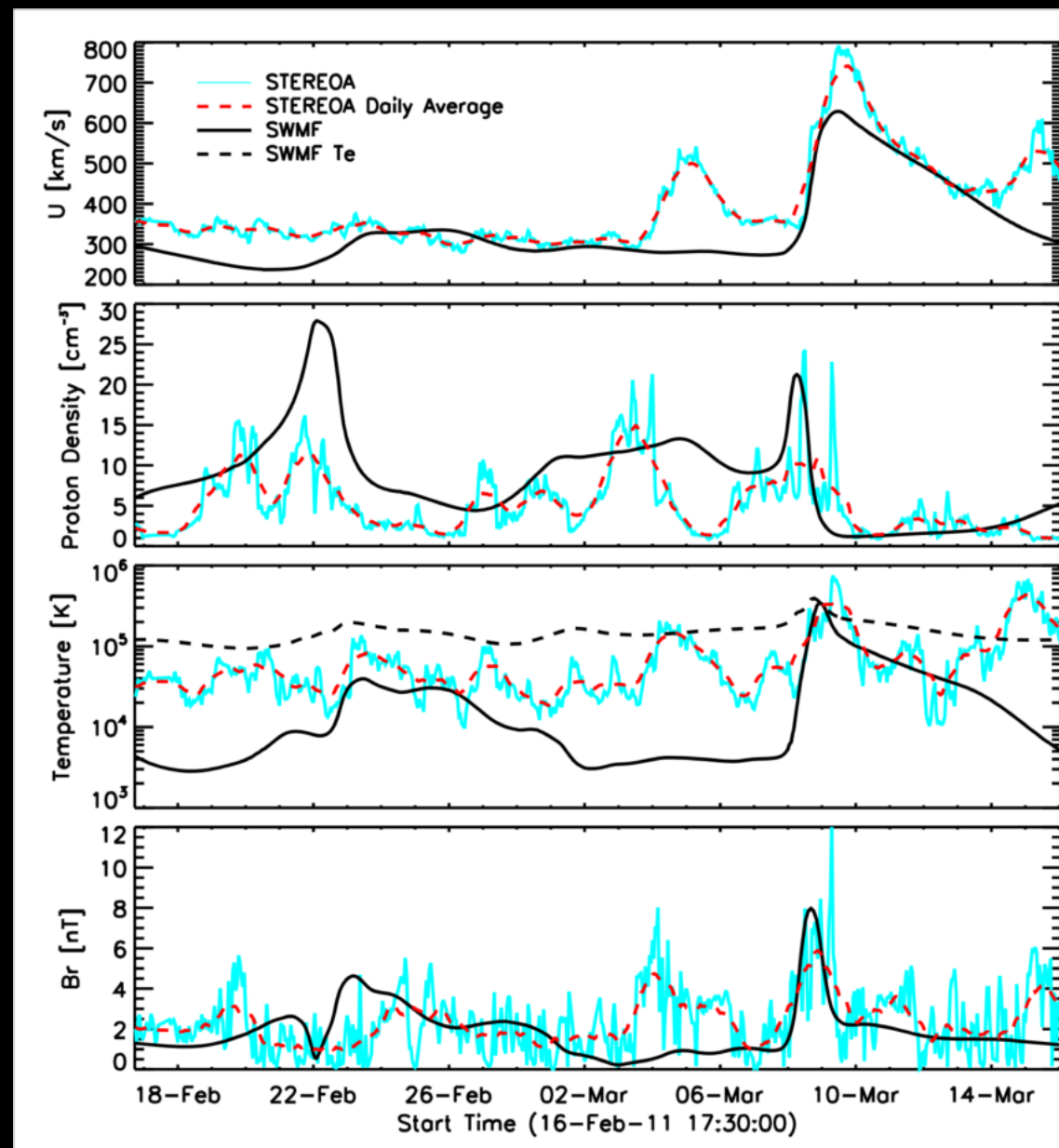
Model Validation near the Sun and at 1 AU

Model-Observation Comparison in EUV

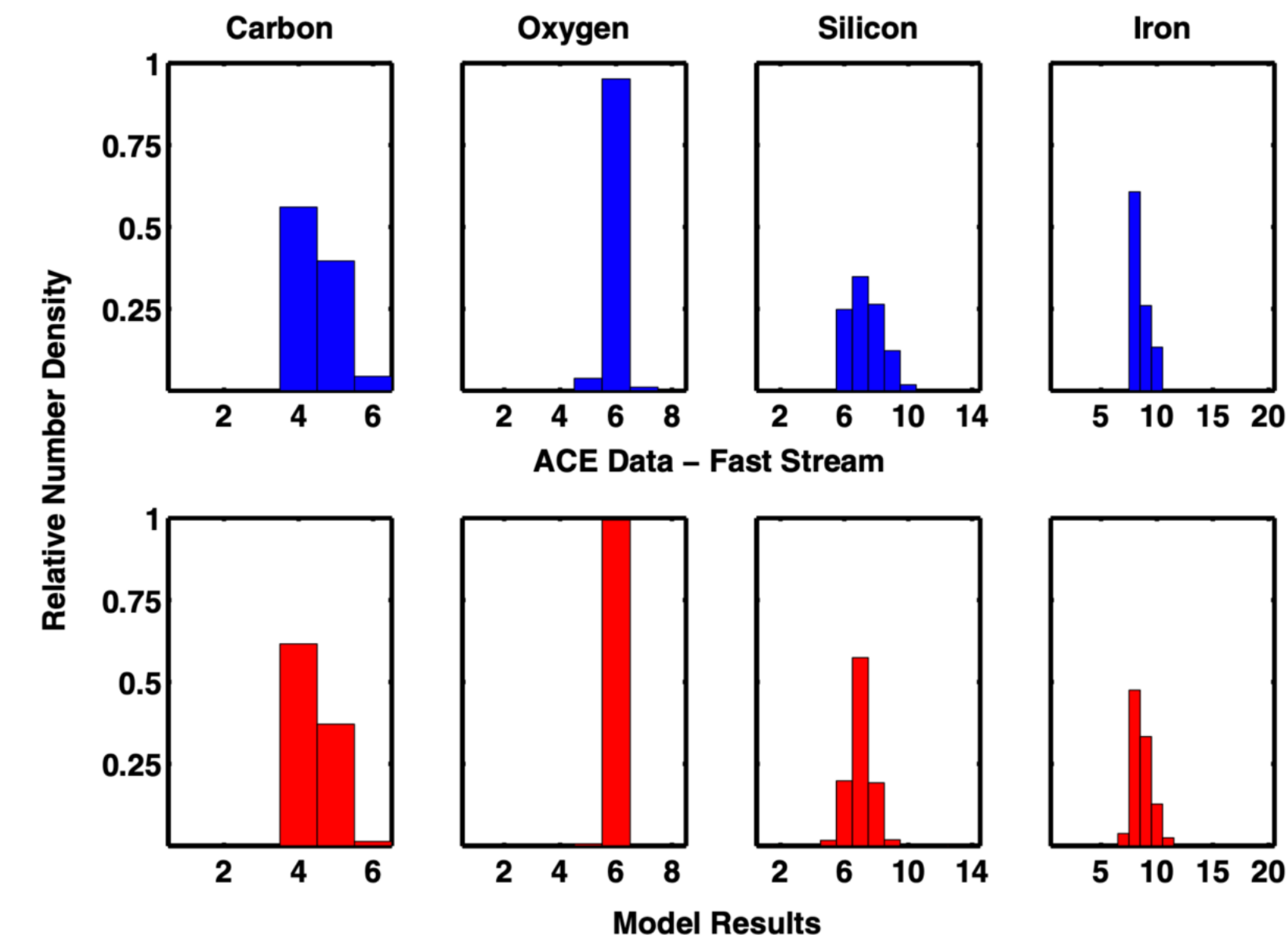


Jin et al. 2017a

Plasma Parameters at 1 AU



Ion-Charge State Comparison

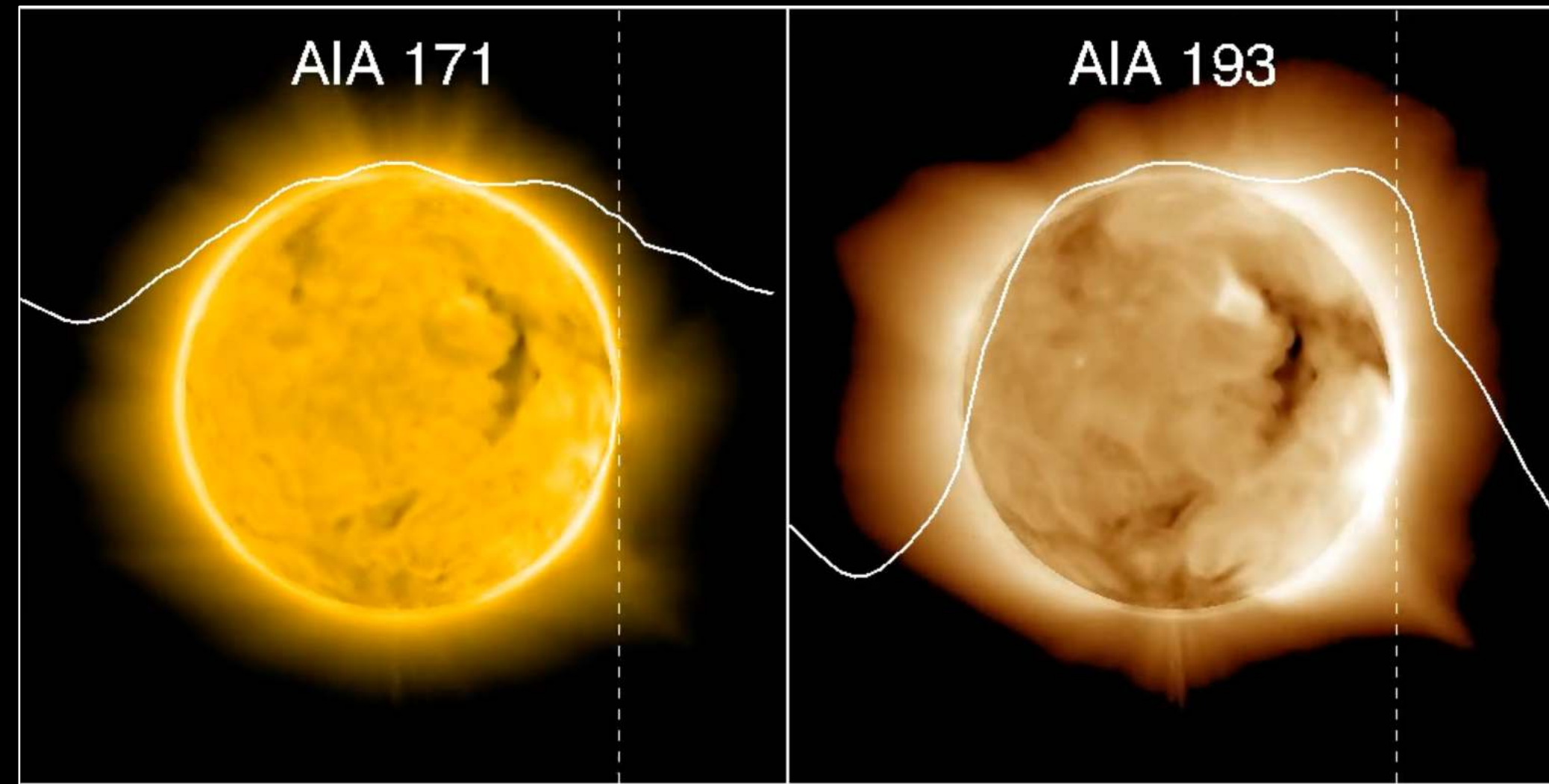


Jin et al. 2012

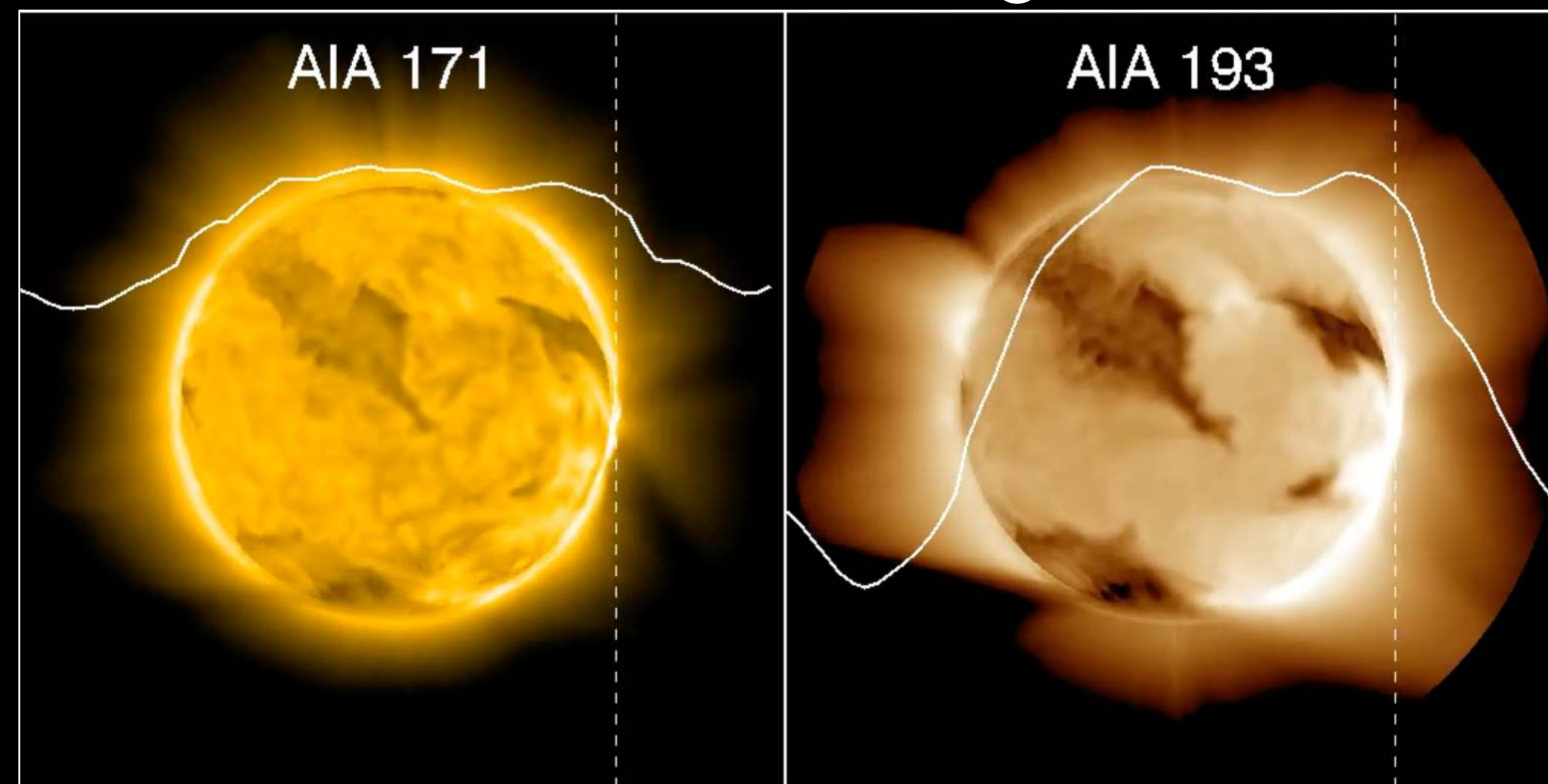
- Ionic Charge State Calculation: solar wind model's **electron temperature** and **density** as inputs to **the ionic charge state equation**, while the model **velocity** as input into **the continuity equation** (Gruesbeck et al. 2011, Landi et al. 2012).

MUSE Science: Constrain Alfvén Wave Heating Parameters

Reduced Heating Case

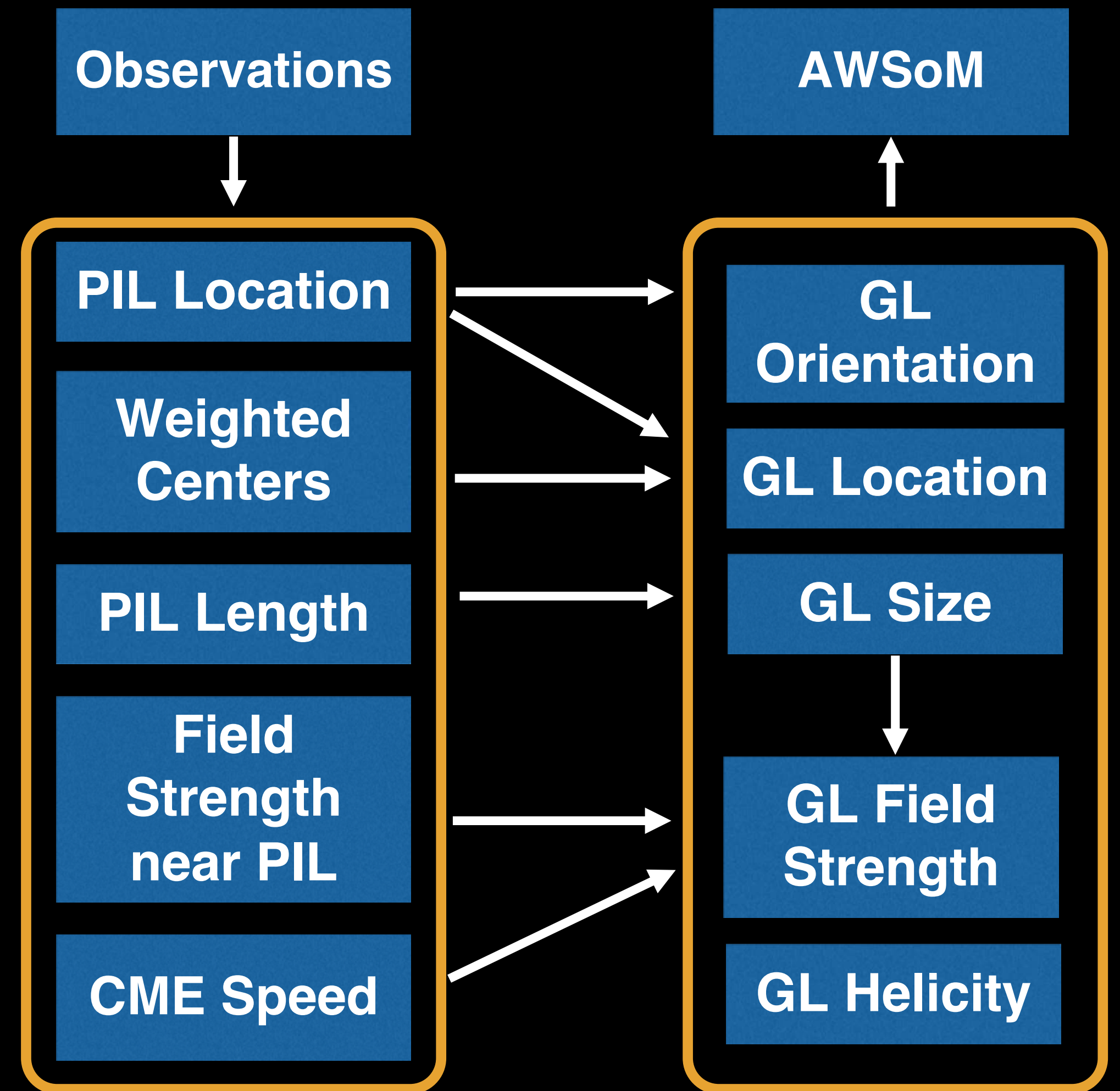
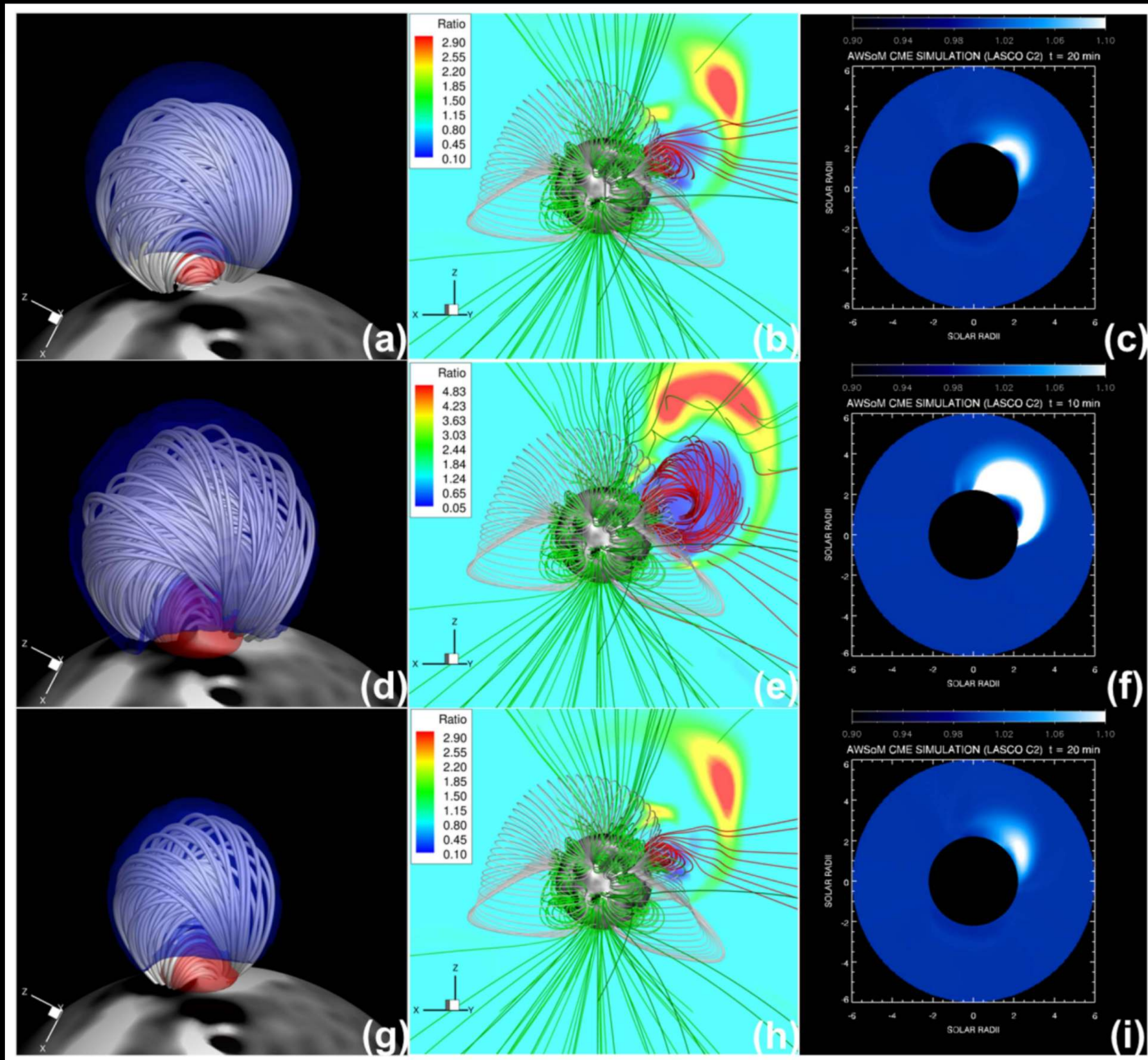


Enhanced Heating Case



- Current global MHD models based on Alfvén wave heating use a uniform **mean velocity amplitude of Alfvén waves** (δU) at the inner boundary that determines energy input into the solar atmosphere.
- The coronal heating parameters in the model can significantly influence the global corona and background solar wind solution.
- **MUSE observations will provide spatially resolved δU measurement (i.e., non-thermal line broadening) as well as constrain the wave energy dissipation process.**

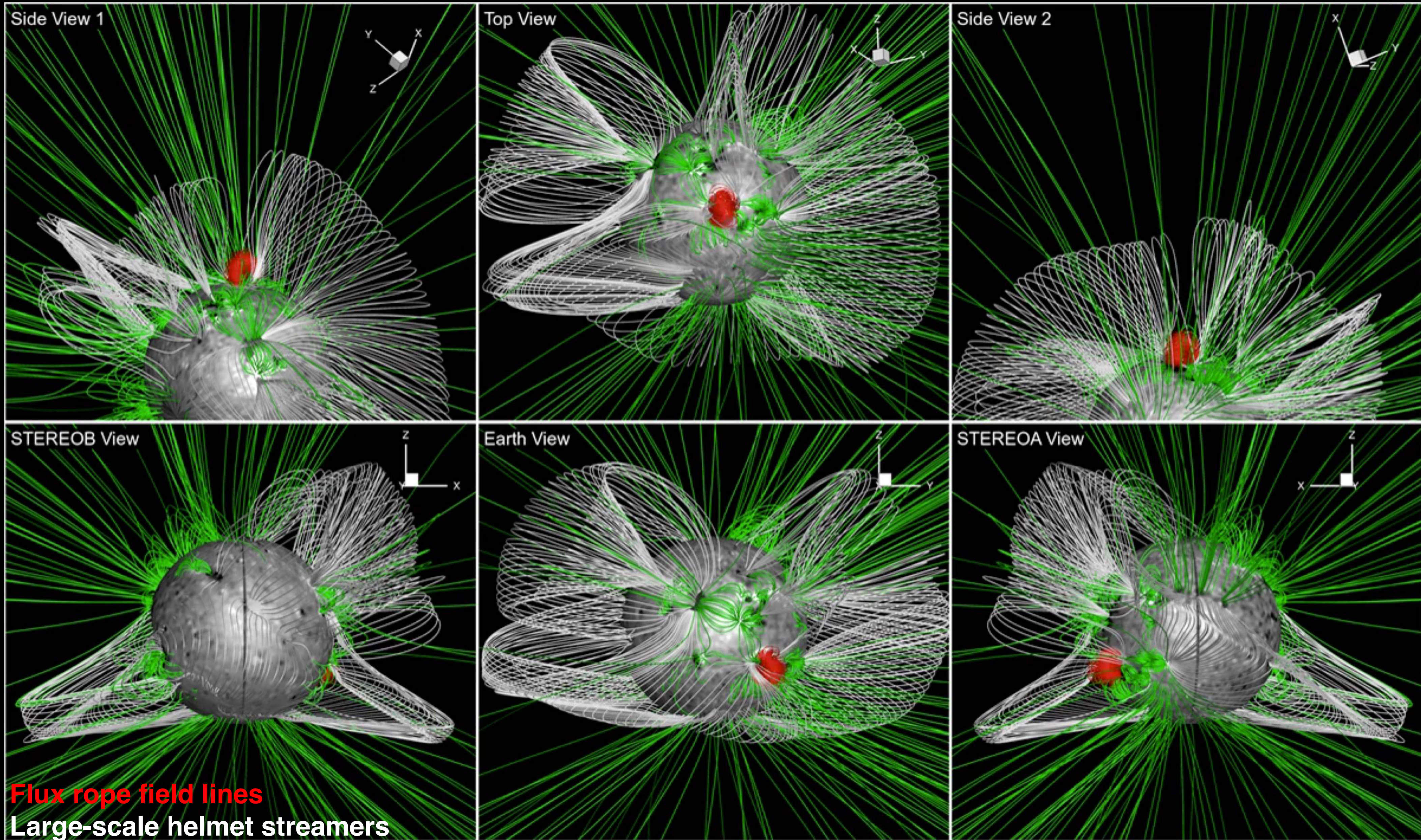
EEGGL: Eruptive Event Generator (Gibson and Low)



(Jin et al. 2017b)

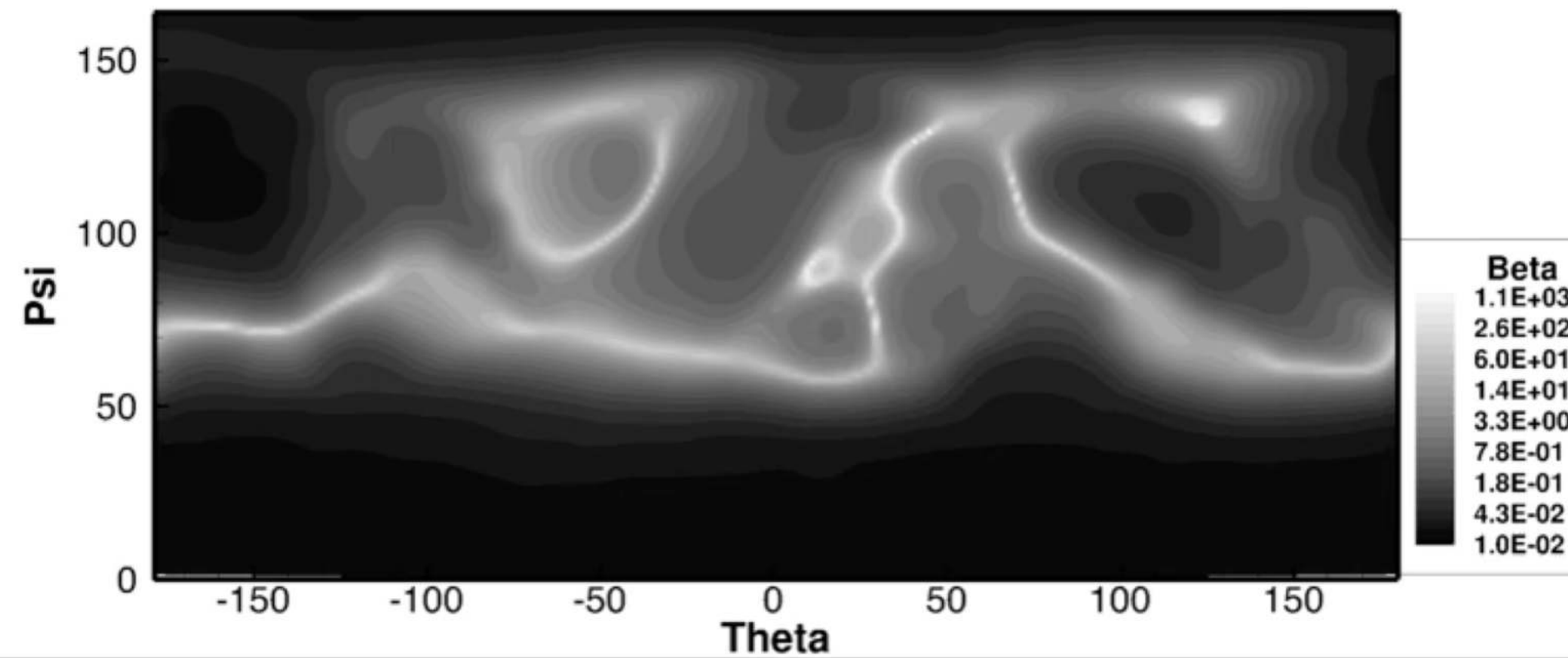
More information: <https://ccmc.gsfc.nasa.gov/tools/eeggl/>

3D Field Evolution in 1 Hour



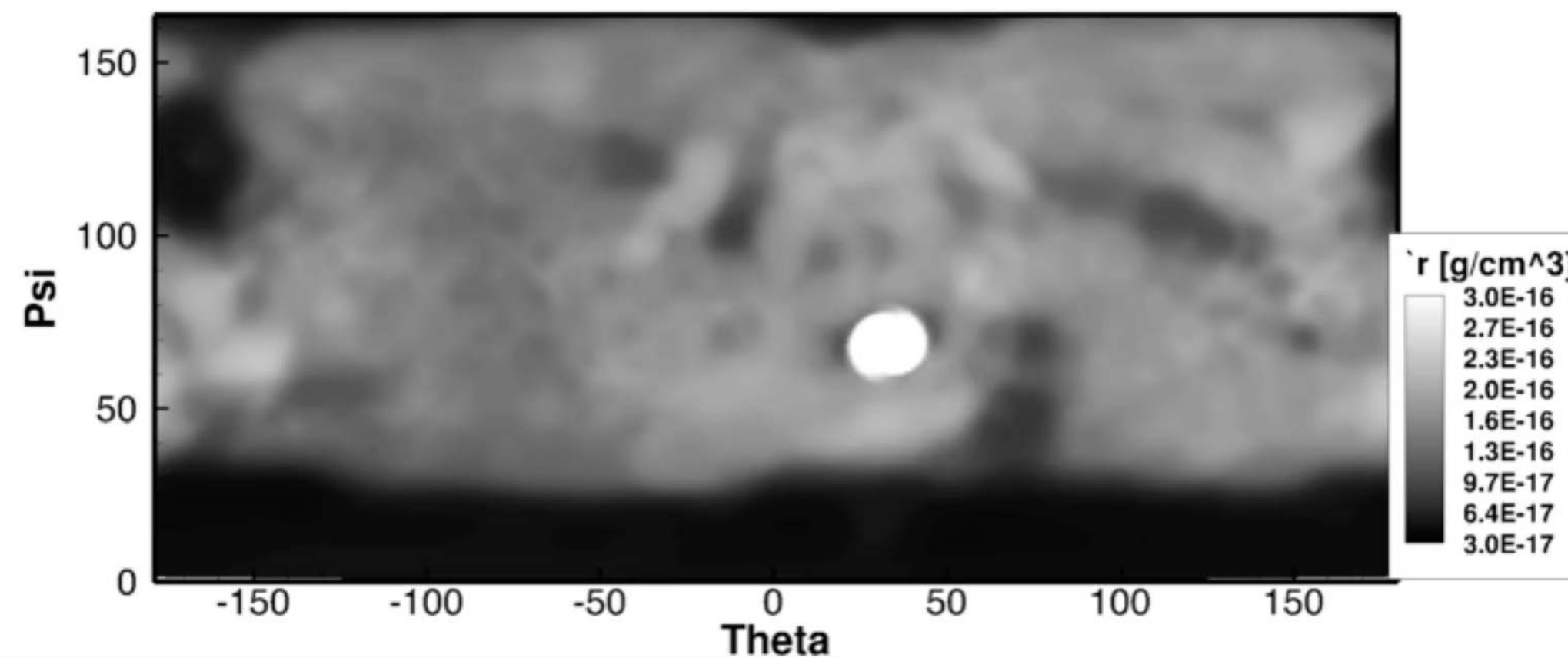
Plasma Beta

- Plasma beta at **2.5 Rs**
- The eruption changes the current sheet location therefore the large-scale magnetic configuration significantly.



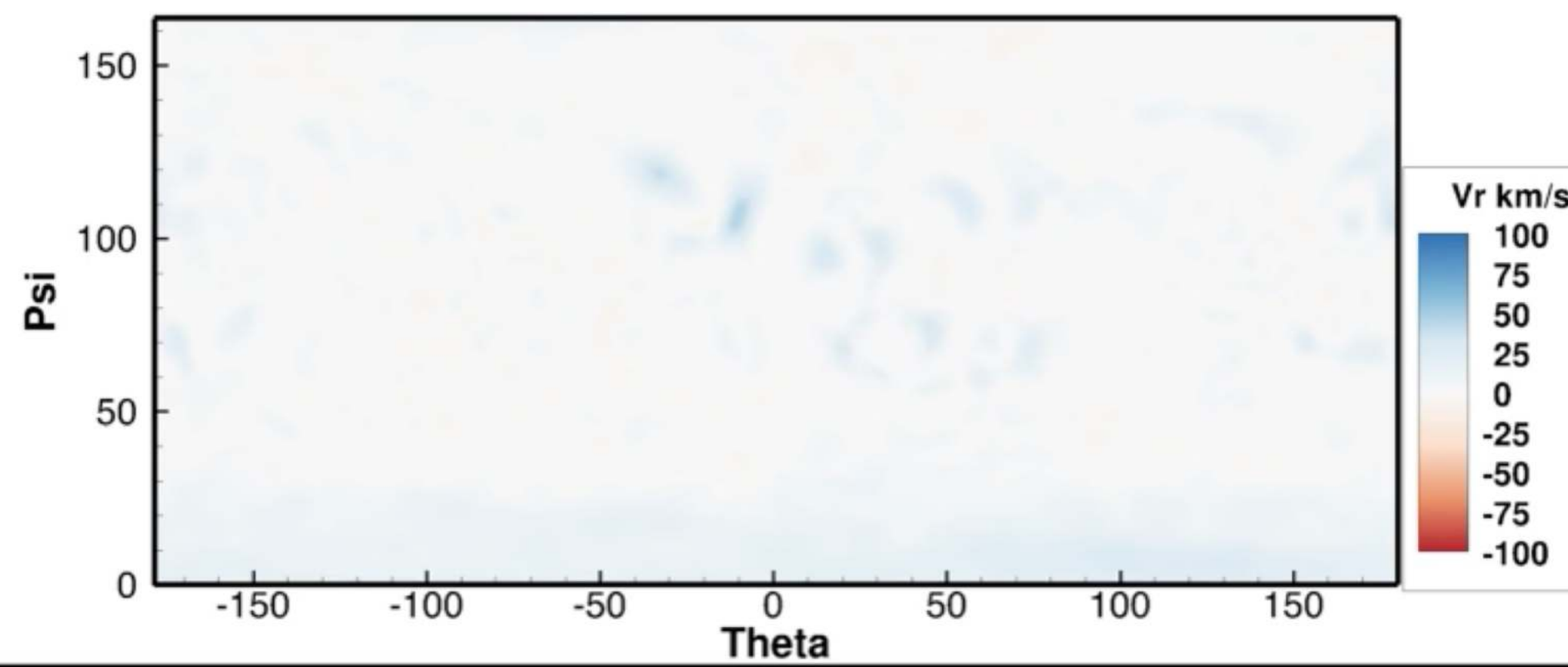
Plasma Density

- Plasma density at **42 Mm**
- Waves reflection from the north and south polar coronal hole boundary.



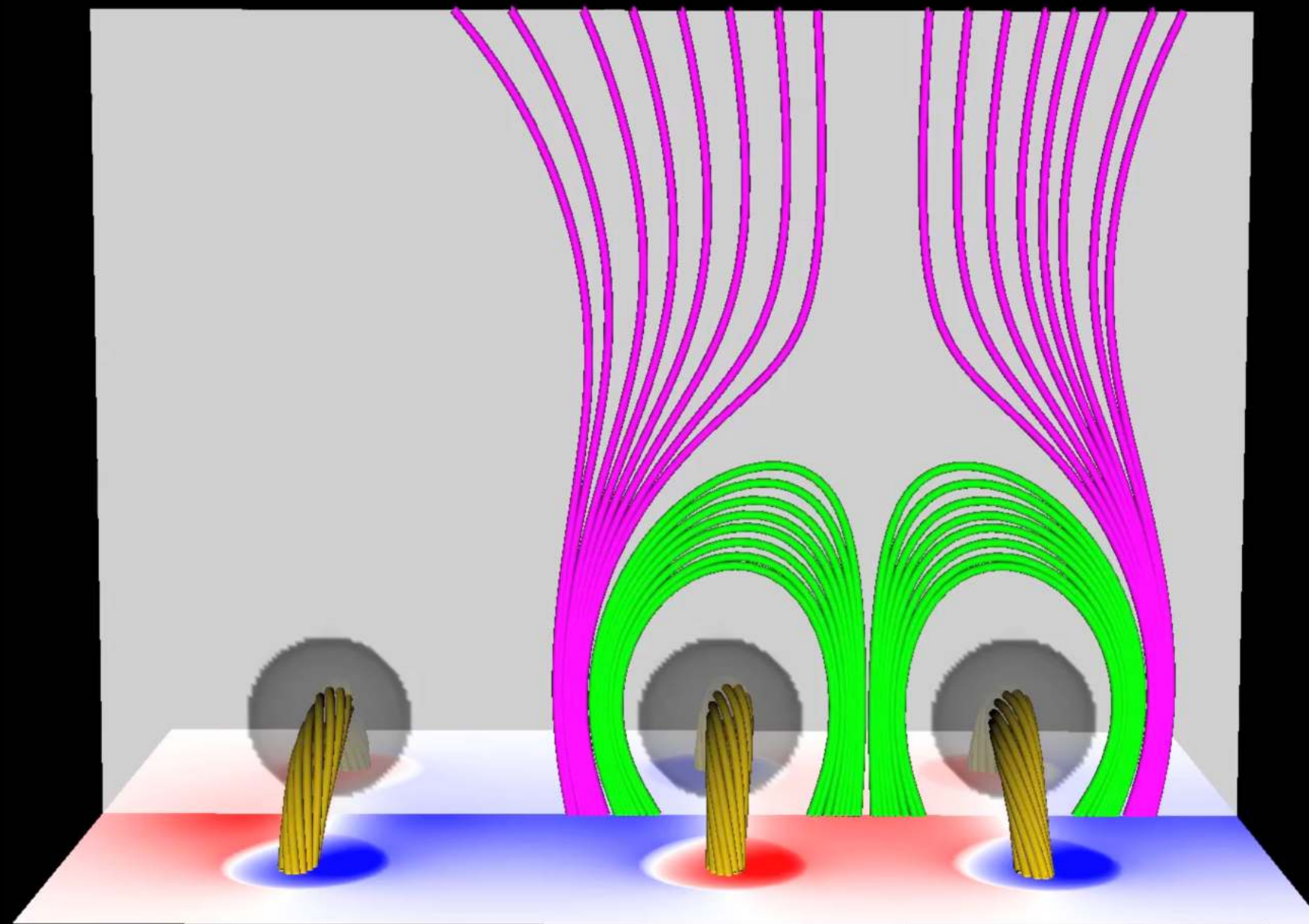
Dopplergram

- Radial velocity at **42 Mm**
- Downward flow due to the expansion of the CME.

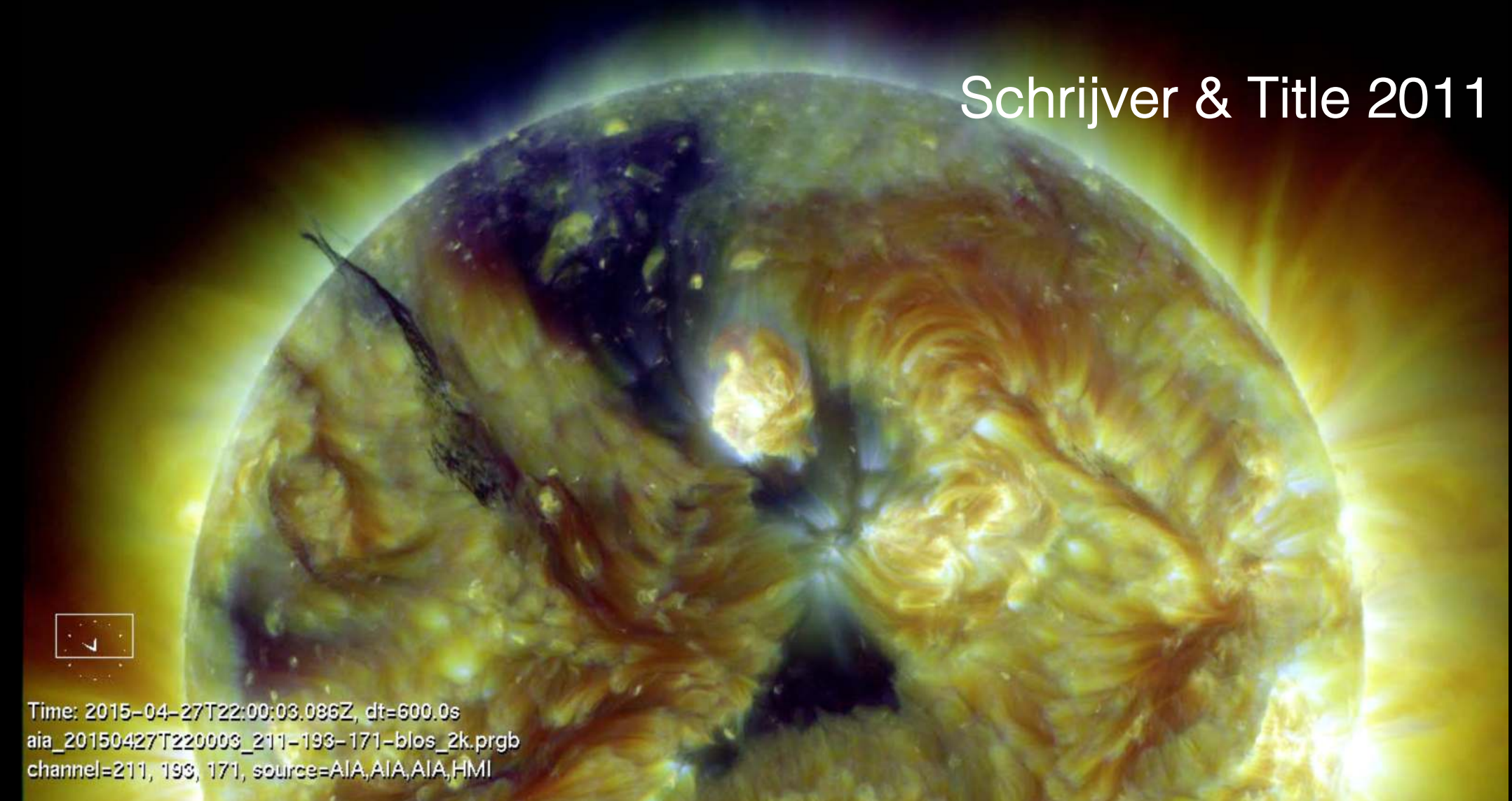


Solar Sympathetic Eruptions

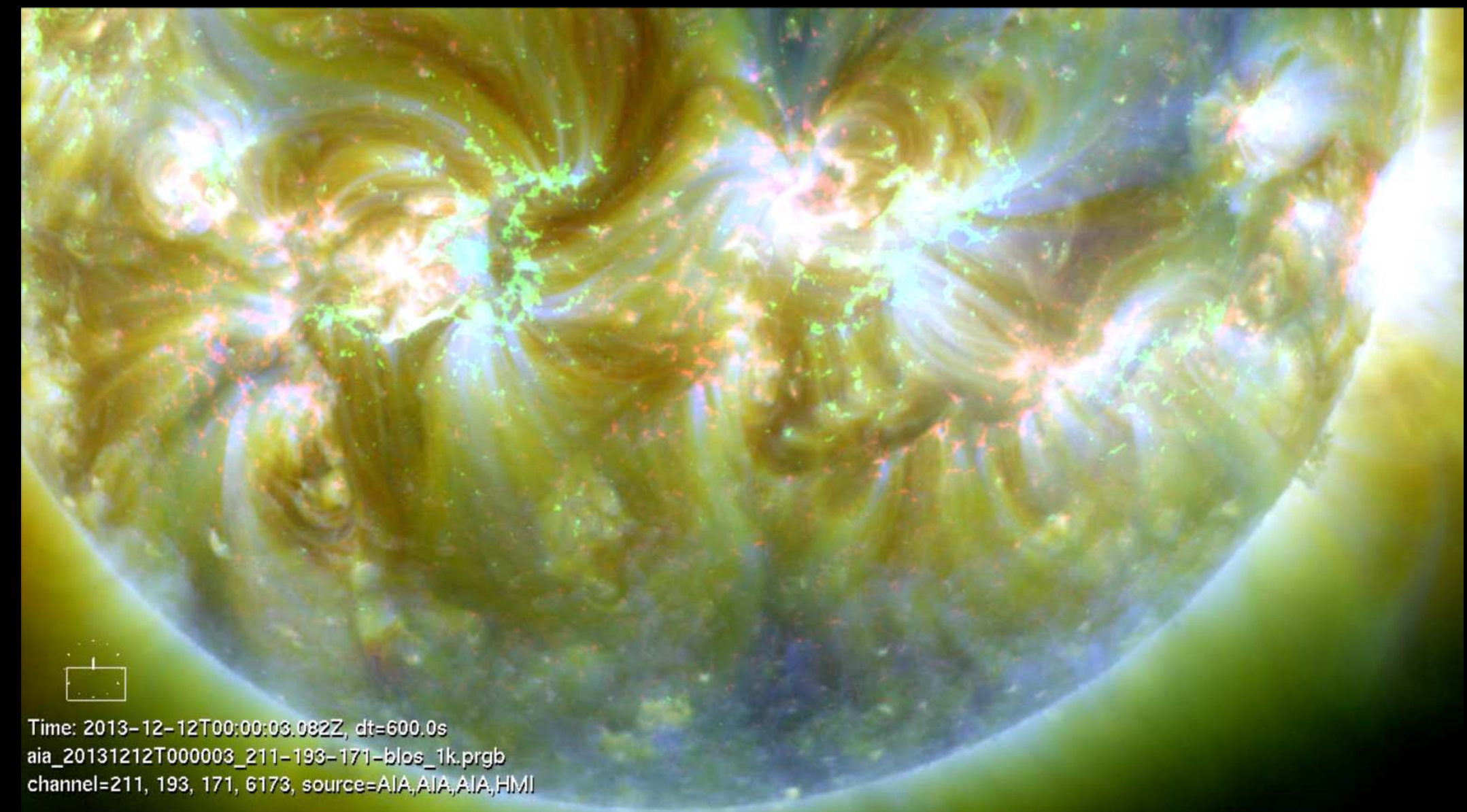
- There are statistical studies suggest the existence of solar sympathy (e.g., Schrijver et al. 2015, Fu & Welsch 2015).
- Comparing with the initiation mechanisms of “isolated” events, the mechanisms for sympathetic events are less understood (Schrijver & Title 2011, Torok et al. 2011, Titov et al. 2012, Lynch & Edmondson 2013).

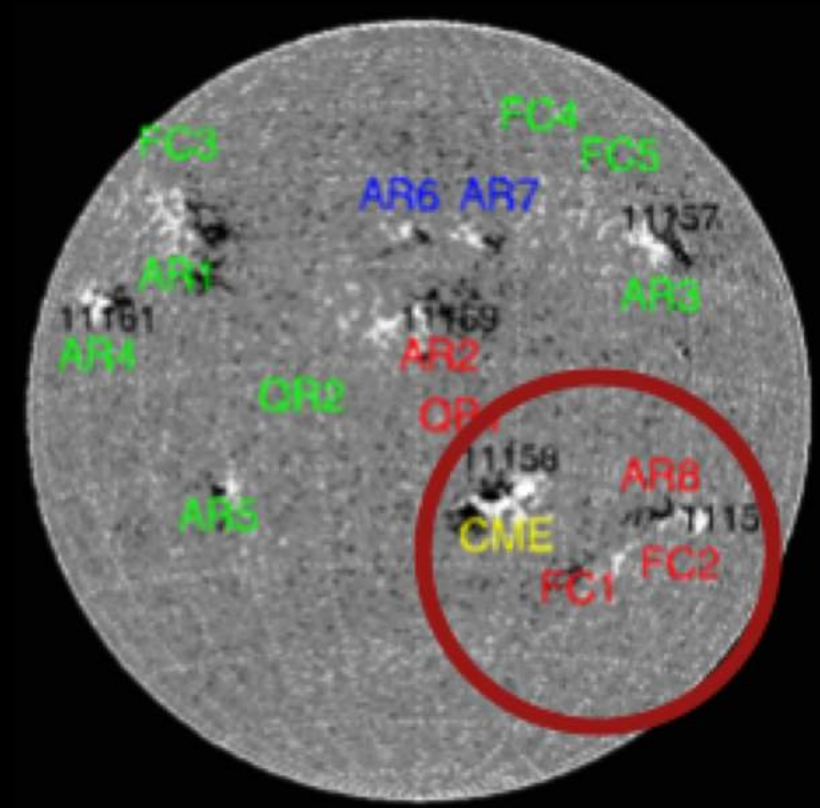
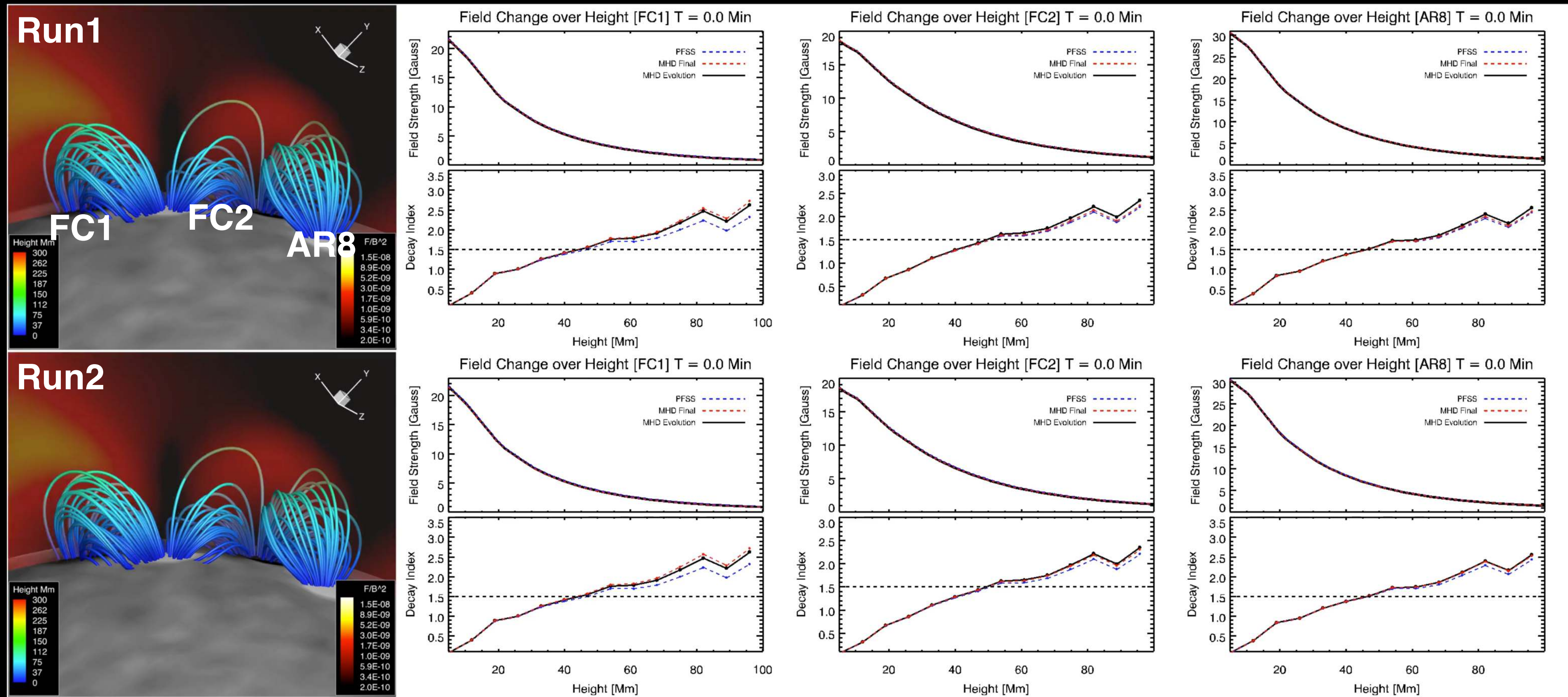


Torok et al. (2011) reproduce some important aspects of the global sympathetic event and suggests the importance of the pseudo-streamer for producing the “twin-filament” eruptions.



Schrijver & Title 2011





- The **critical decay index**, above which the flux rope becomes unstable due to torus instability, depends on the flux rope configuration (1.0 for a straight line current, 1.5 for a toroidal current).
- Our study suggests that **the expansion-induced reconnection** (van Driel-Gesztelyi et al. 2014) may provide a primary coupling mechanism of sympathetic eruptions.
- **The erupting flux rope configuration can significantly influence the impact magnitude.**

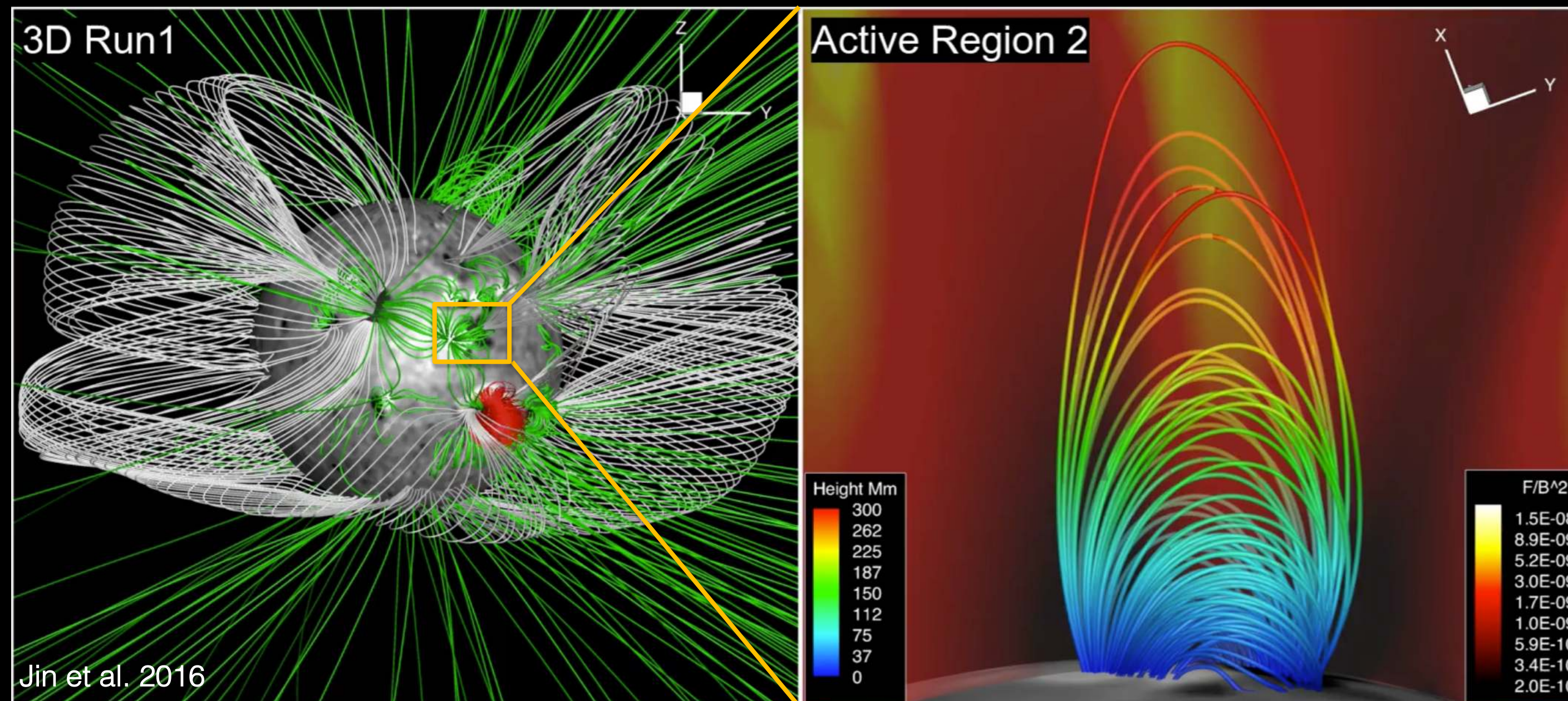
MUSE Science: CME Interaction with Solar Atmosphere

Global MHD Simulation of a CME Eruption & Disrupted Coronal Structure

Red:
CME Flux Rope

White:
Global helmet
streamers

Green:
Field line from
surrounding
active regions
and open field.

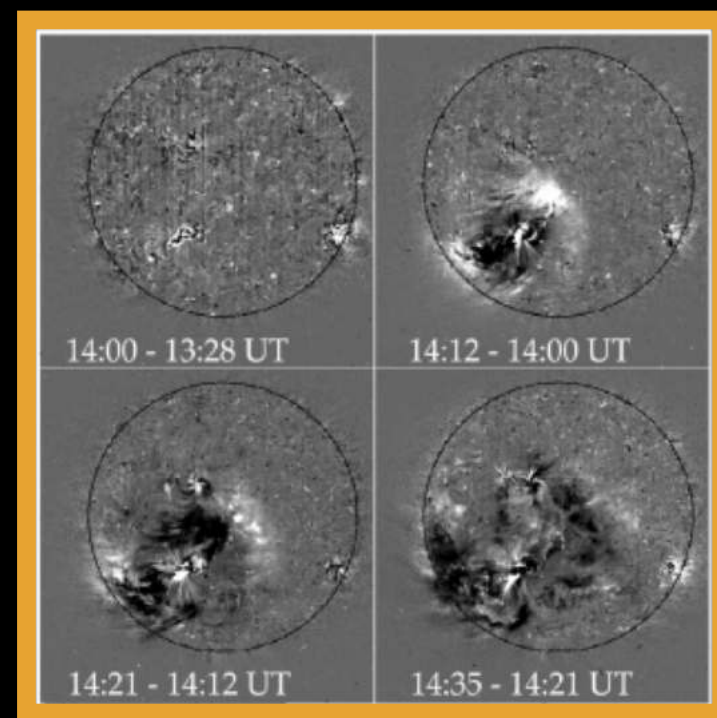


The high temporal and spatial resolution spectral observation enabled by MUSE can significantly advance our understanding about how CME interact with global solar atmosphere and how CME perturbations propagate from one region to another to trigger an eruption.

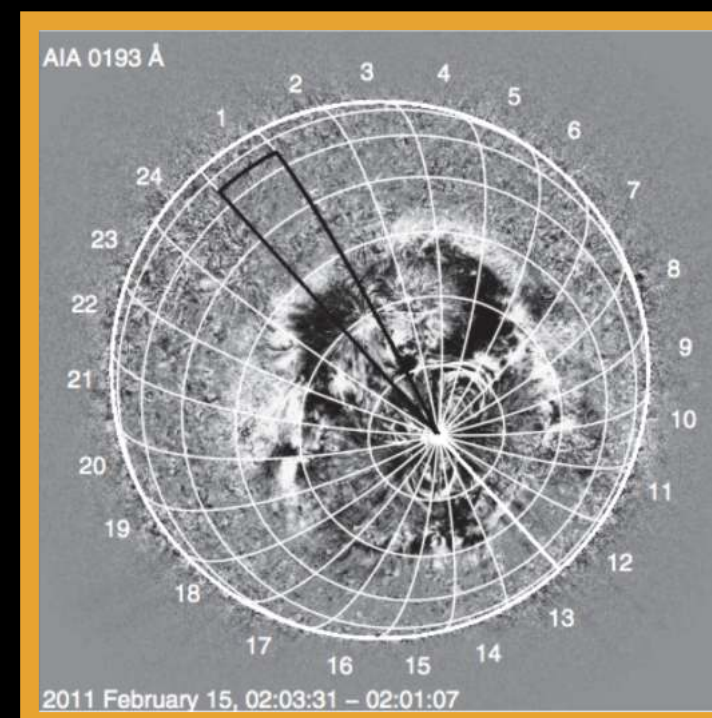
- After the eruption, CMEs start to interact with the global solar corona, which can change large-scale corona structures, and in some cases trigger a distance region to erupt (i.e., **sympathetic solar events**: Schrijver & Title, 2011).
- This process is mainly observed through EUV imagers without spectral information. Even for a handful events with spectral data available (Harra et al. 2011; Chen et al. 2011), the temporal resolution is insufficient to catch up the details of the interaction process (time scale of seconds to minutes).

Coronal Dimming & EUV Waves

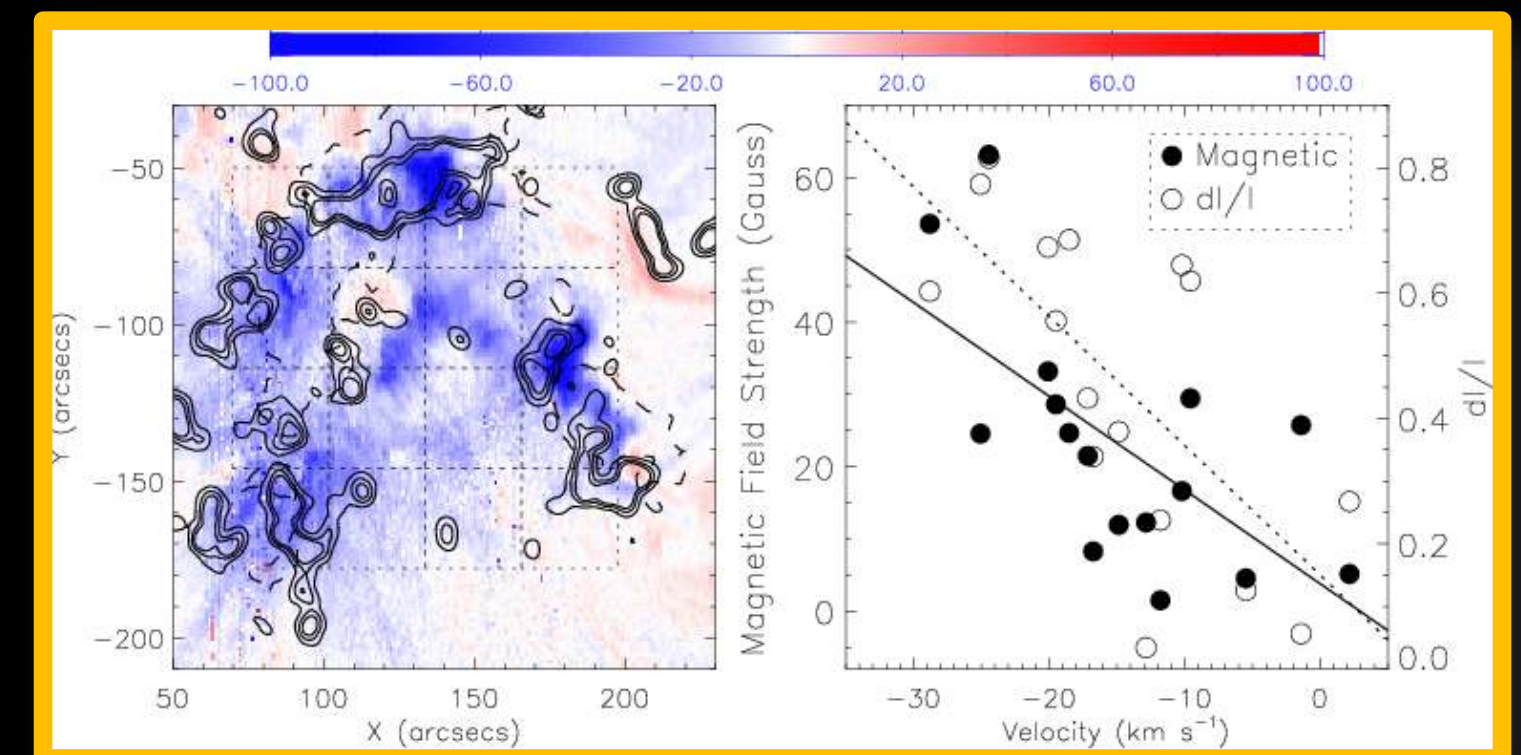
- Coronal dimming is **the reduction in intensity** on/near the solar disk across a large area, which has been observed in many wavebands (e.g., white-light, X-ray, EUV) of solar observation. And it is usually associated with **coronal EUV waves**.
- Spectroscopic observations confirmed that the dimmings are regions of **up-flowing expanding plasma** (e.g., *Harra & Sterling, 2001, Harra et al. 2007, Imada et al. 2007, Jin et al. 2009, Attril et al. 2010, Tian et al. 2012*). Both observation and MHD Modeling of solar coronal dimming (e.g., *Cohen et al. 2009, Downs et al. 2012*) suggest that the coronal dimming is mainly caused by the **CME-induced plasma evacuation**, and the spatial location is well correlated with **the footpoints of the erupting magnetic flux system** (*Downs et al. 2015*).
- **Solar observations suggest that all coronal dimmings were associated with CMEs**. Therefore, they might encode important information about CME's mass, speed, energy etc. (e.g., *Hudson et al. 1996, Sterling & Hudson 1997, Harrison et al. 2003, Zhukov & Auchere 2004, Aschwanden et al. 2009, Cheng & Qiu 2016, Krista & Reinard 2017*).
- *Harra et al. (2016)* found “**coronal dimming is the only signature that could differentiate powerful flares that have CMEs from those that do not**”. Therefore, dimming might be one of the best candidates to observe the CMEs on distant Sun-like stars (*Veronig et al. 2021, Loyd et al. 2022*).



EUV Dimming by SOHO/EIT
(Thompson et al. 1999)



EUV Dimming by SDO/AIA
(Nitta et al. 2013)

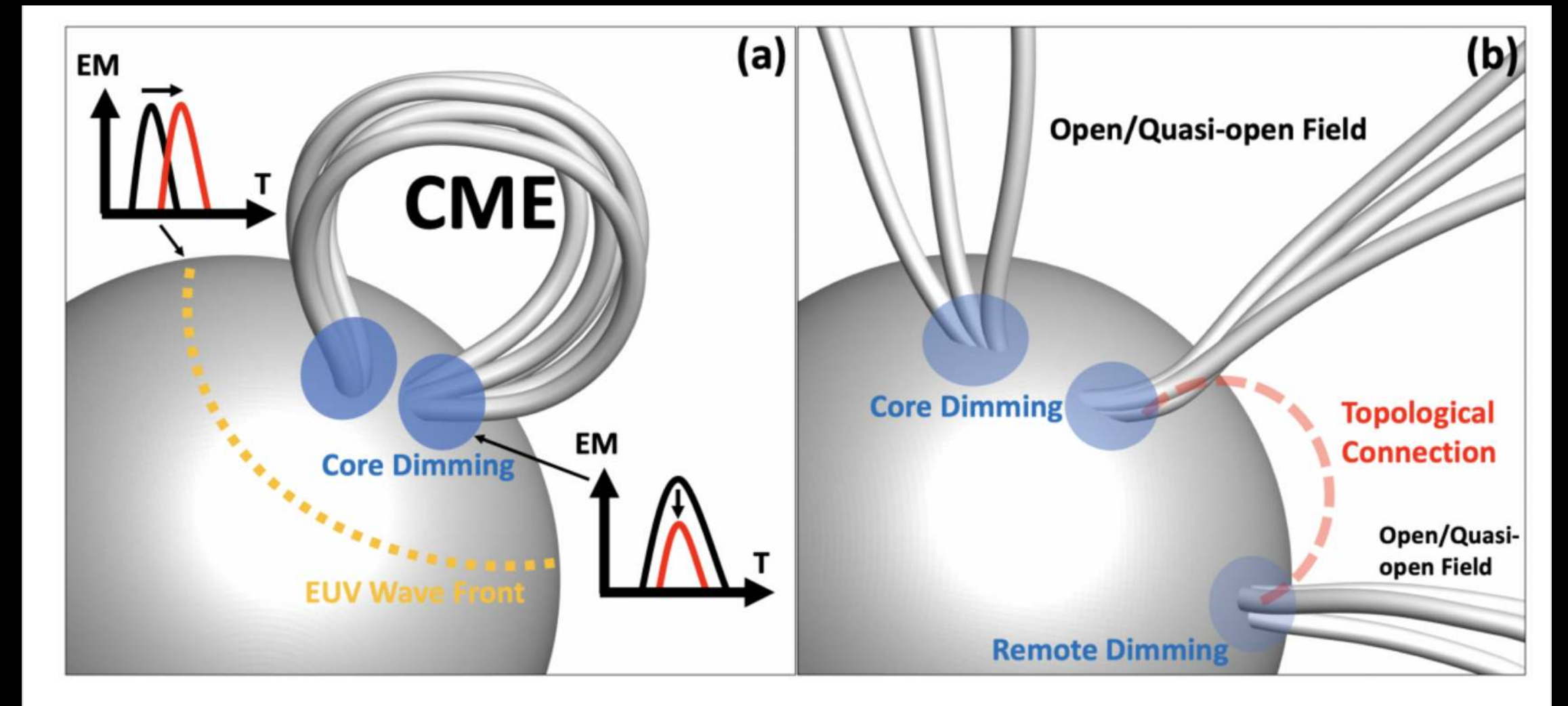
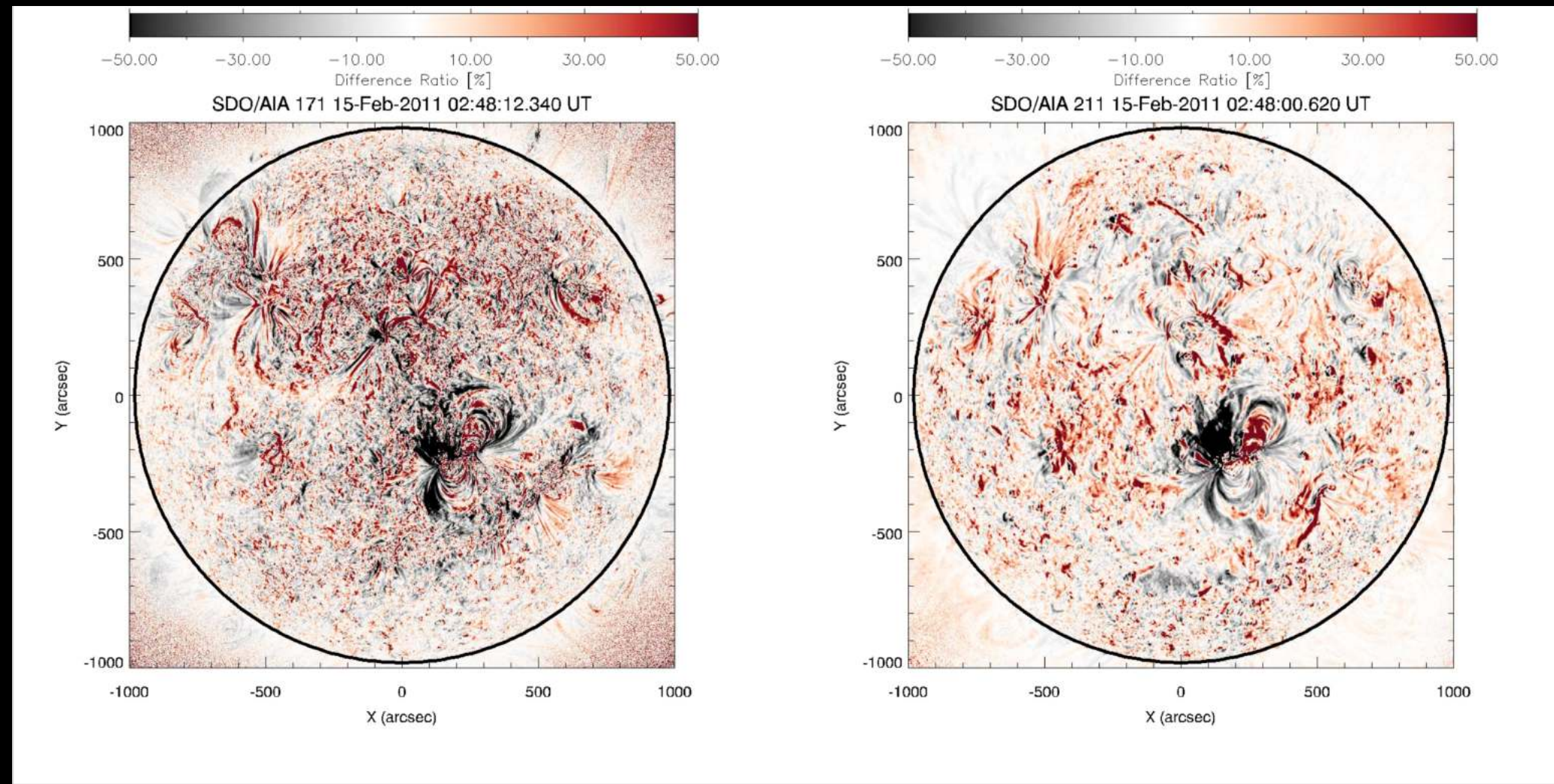


CME-induced Outflow Observed by Hinode/EIS
(Jin et al. 2009)

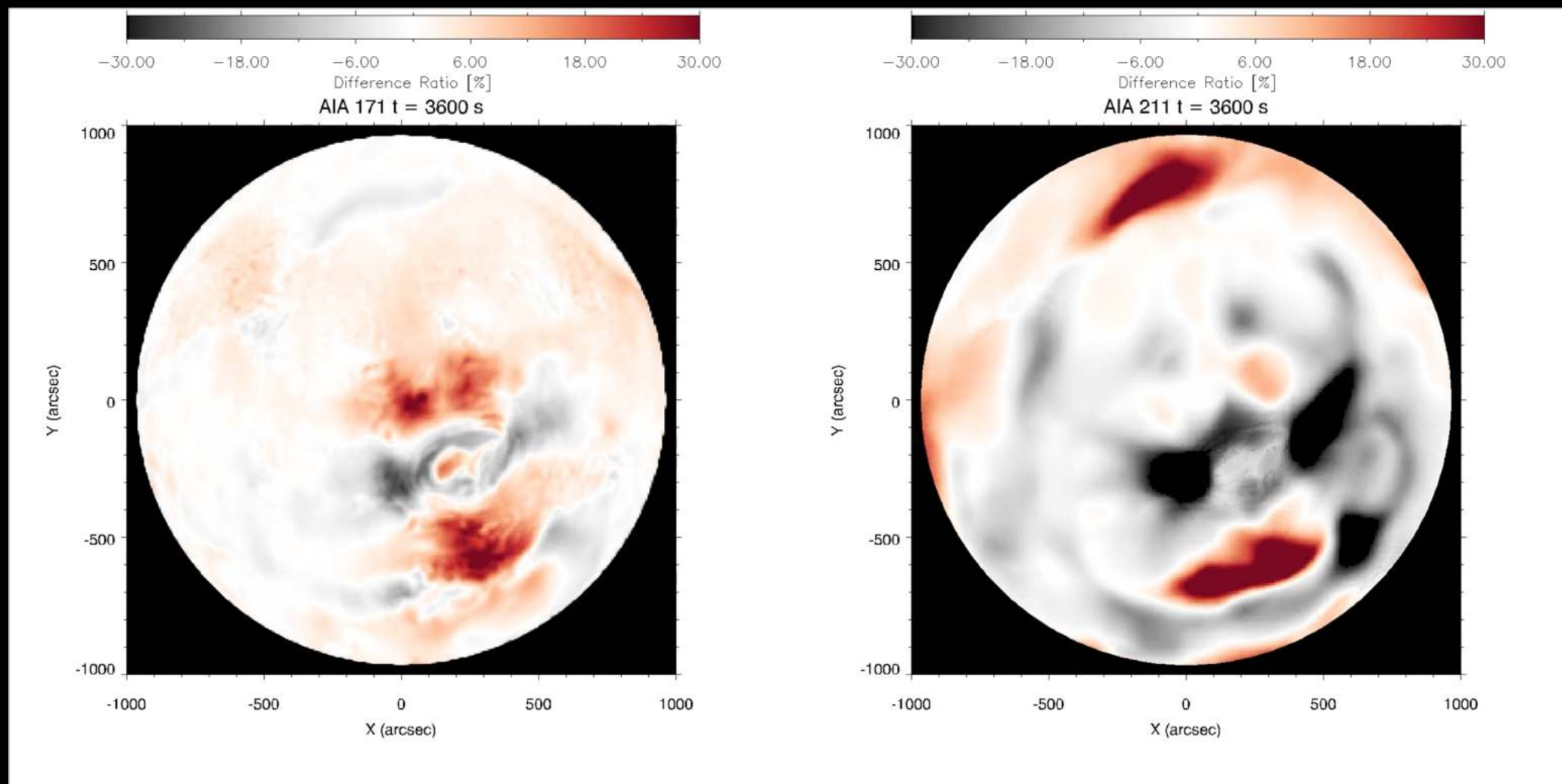
Observed and Simulated Coronal Dimming & EUV Waves

AIA 171 (T = 0.63 MK)

AIA 211 (T = 1.86 MK)



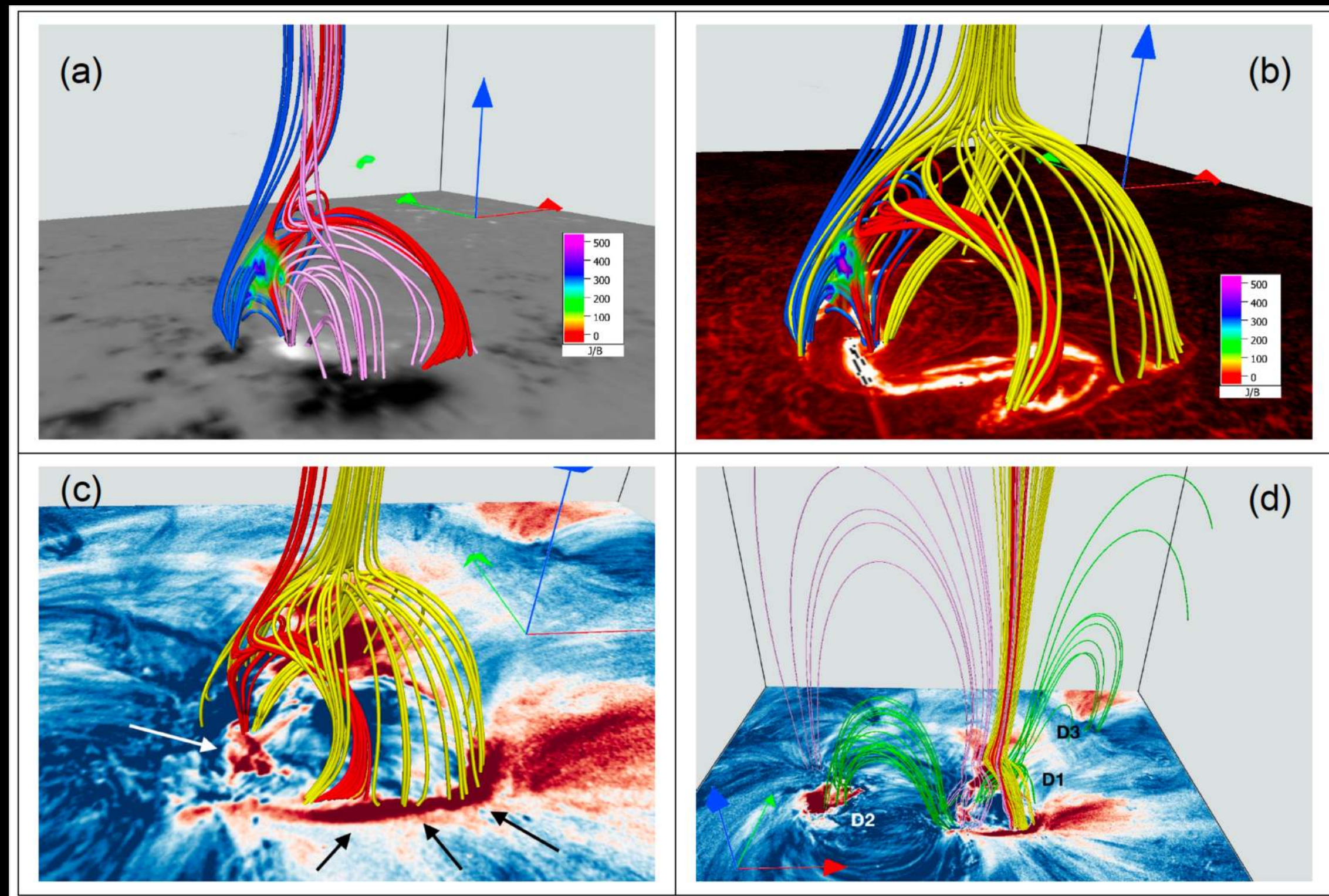
Jin et al. 2022a



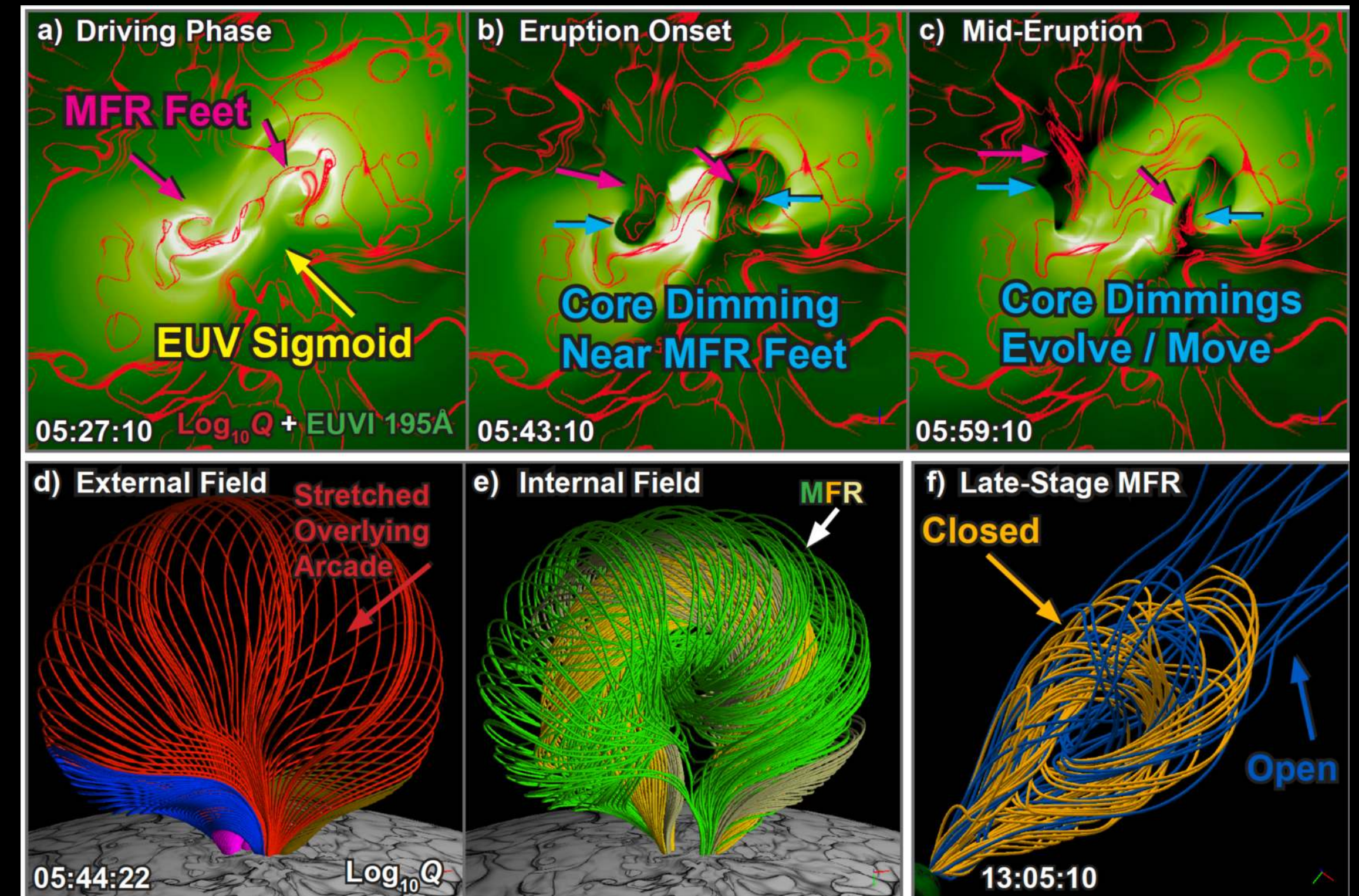
- **Emission Measure (EM)** and **Column Density** calculation from the simulation suggest that both the core and remote dimmings are due to the mass loss induced by the CME.
- Thermal Dimming / brightening of the EUV wave is due to the **plasma compression** during the eruption phase.

Fine Structures and Evolution of Coronal Dimmings

Prasad et al. (2020)



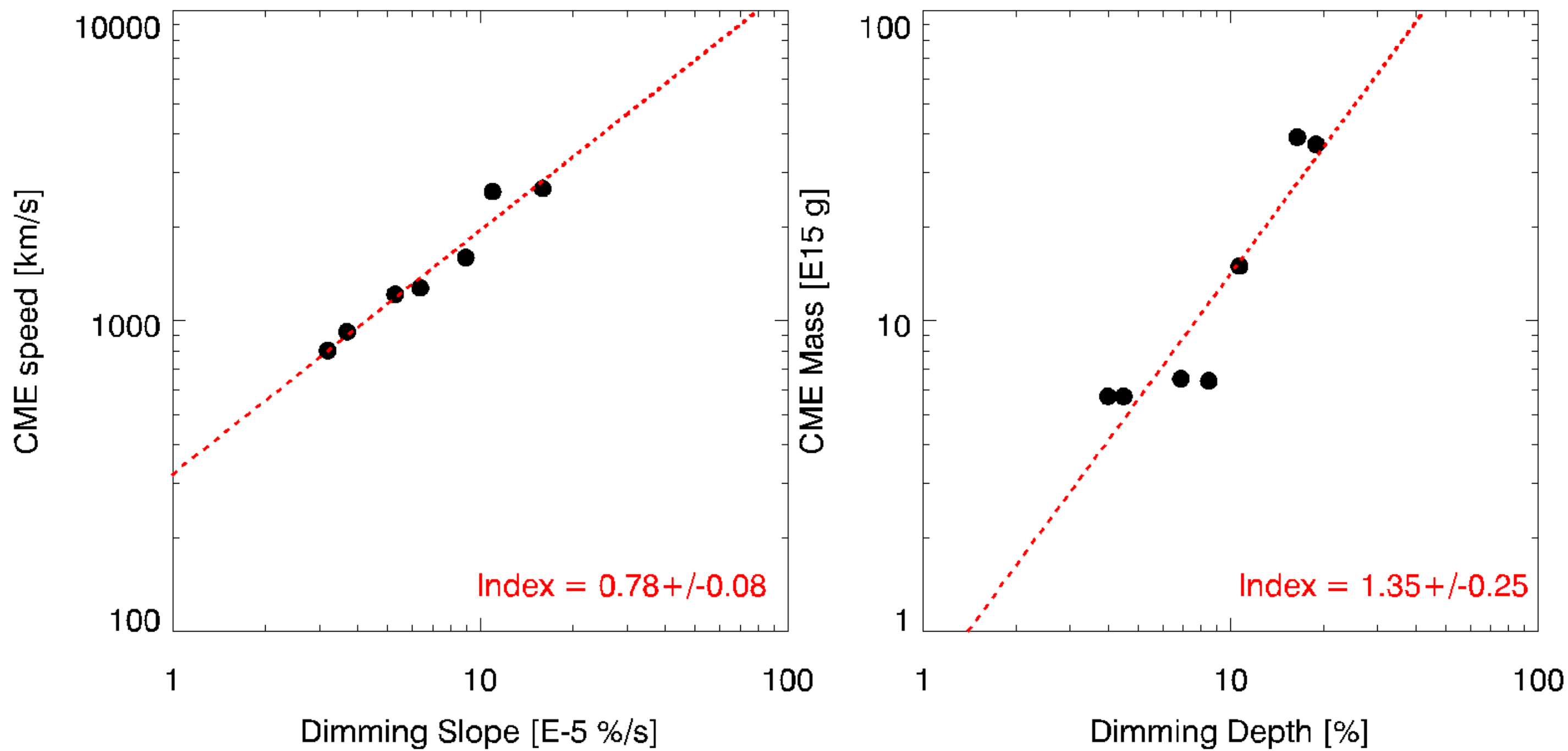
Downs et al. (2023)



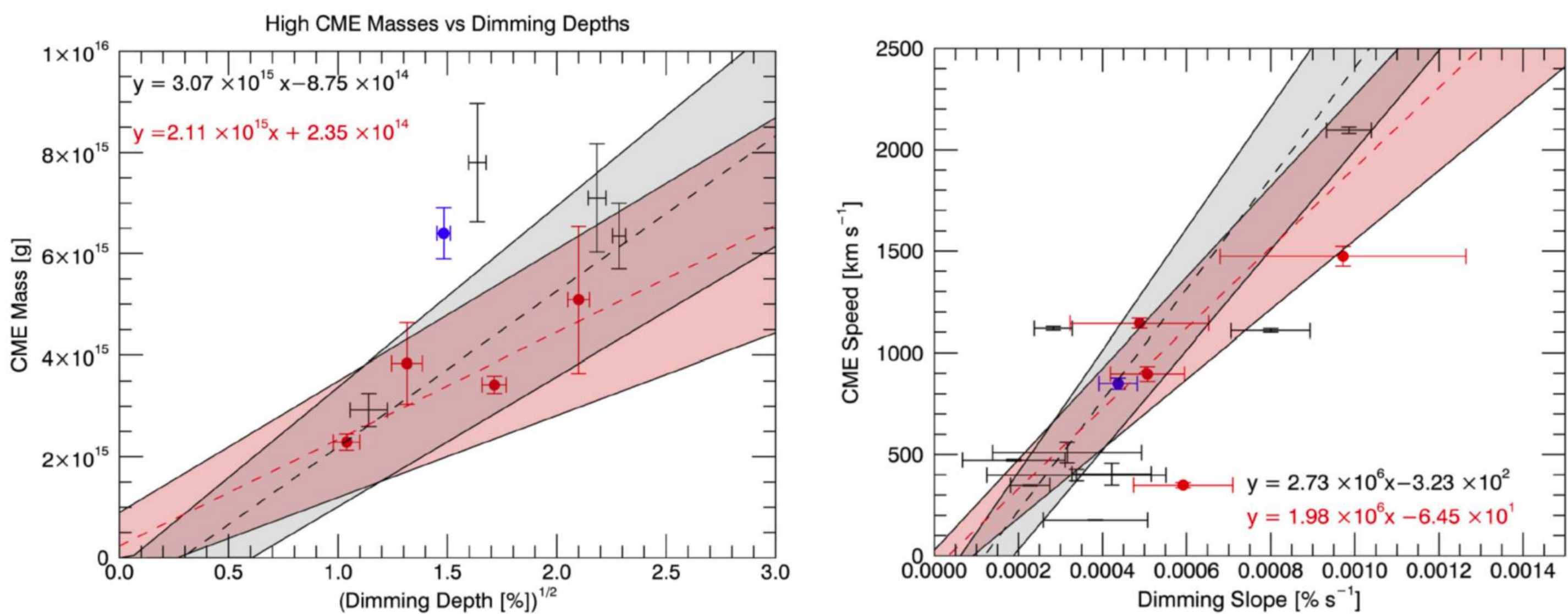
- MHD simulation of the evolution of NOAA AR11283 initiated by an extrapolated **non-force free magnetic field**.
- The footpoints of the 3D null dome surface are co-spatial with the ring-shaped dimming pattern.

- Thermodynamic MHD simulation of the **February 13, 2009** event shows the evolution of core dimmings during the eruption.
- The reconnection between the erupting flux rope and various flux systems results in distinct categories of dimmings (*Upcoming LSRP article by Veronig et al. 2023*).

Coronal Dimming vs. CME Characteristics



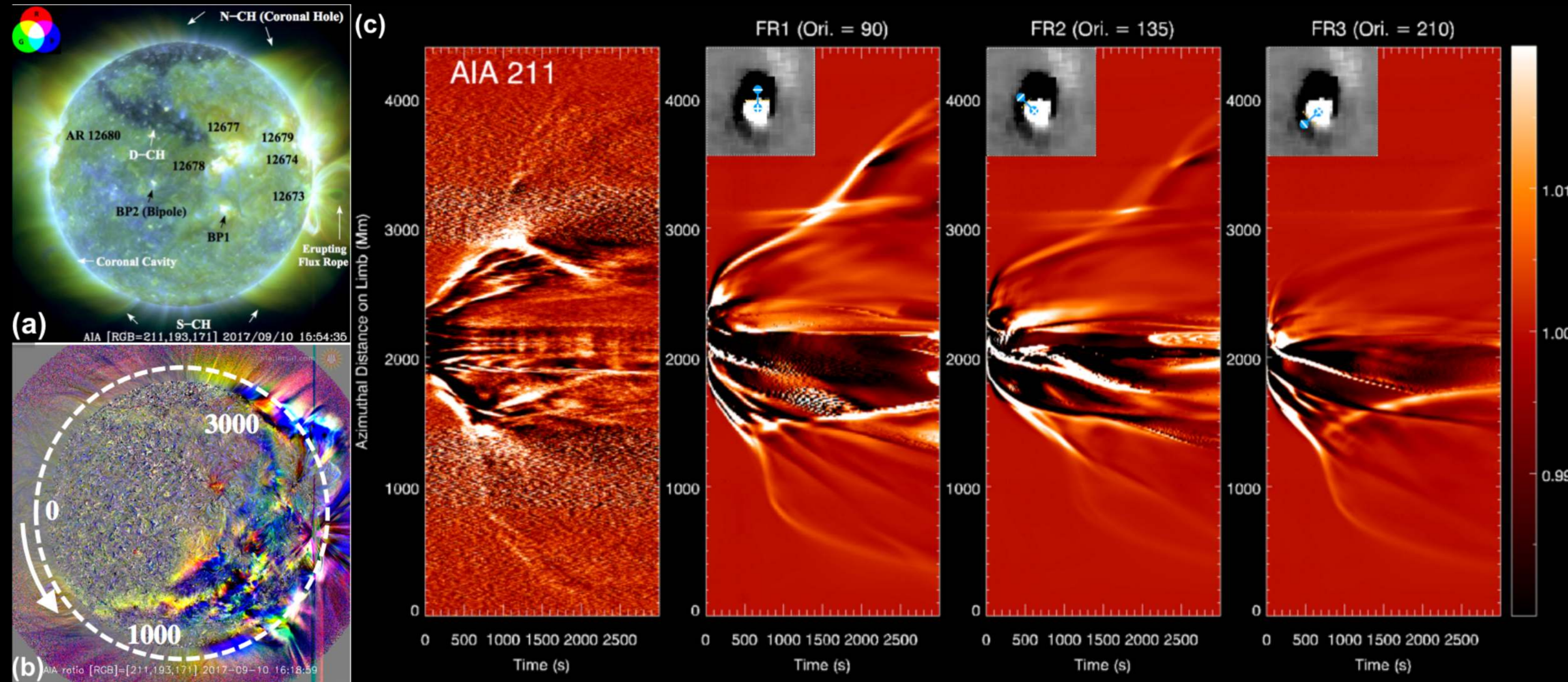
- Note that the simulation runs involve **different flux rope energies** and **flux rope orientations**.
- The simulation result is consistent with the findings of *Mason et al. (2016)* using SDO/EVE observations and *Dissauer et al. (2019)* using SDO/AIA observations.



- CME-induced core dimming occurs much earlier than other associated disturbances (e.g., shocks), the Dimming-CME relationship can provide important estimations about the CME characteristics (e.g., mass, speed) **at the early stage of the eruption.**

MUSE Science: EUV Waves and Coronal Dimmings

2017 September 10 EUV Waves under Different Flux Rope Configurations



Both EUV waves and coronal dimmings are highly correlated with the coronal mass ejections and the erupting magnetic flux ropes associated, the MUSE observation will provide critical information to improve our understanding about these phenomenon as well as their relationship with CMEs into the interplanetary space.

- The MUSE observation on **EUV waves** will provide important diagnosis to understand: How the waves are generated and the interaction with the global solar atmosphere; the relationship between the CME, CME-driven shocks, and EUV waves, etc.
- The MUSE observation on **coronal dimmings** will help to distinguish different dimming types therefore better understanding on the CME-dimming relationship as well as the magnetic reconnection processes between the erupting flux rope and the ambient corona.

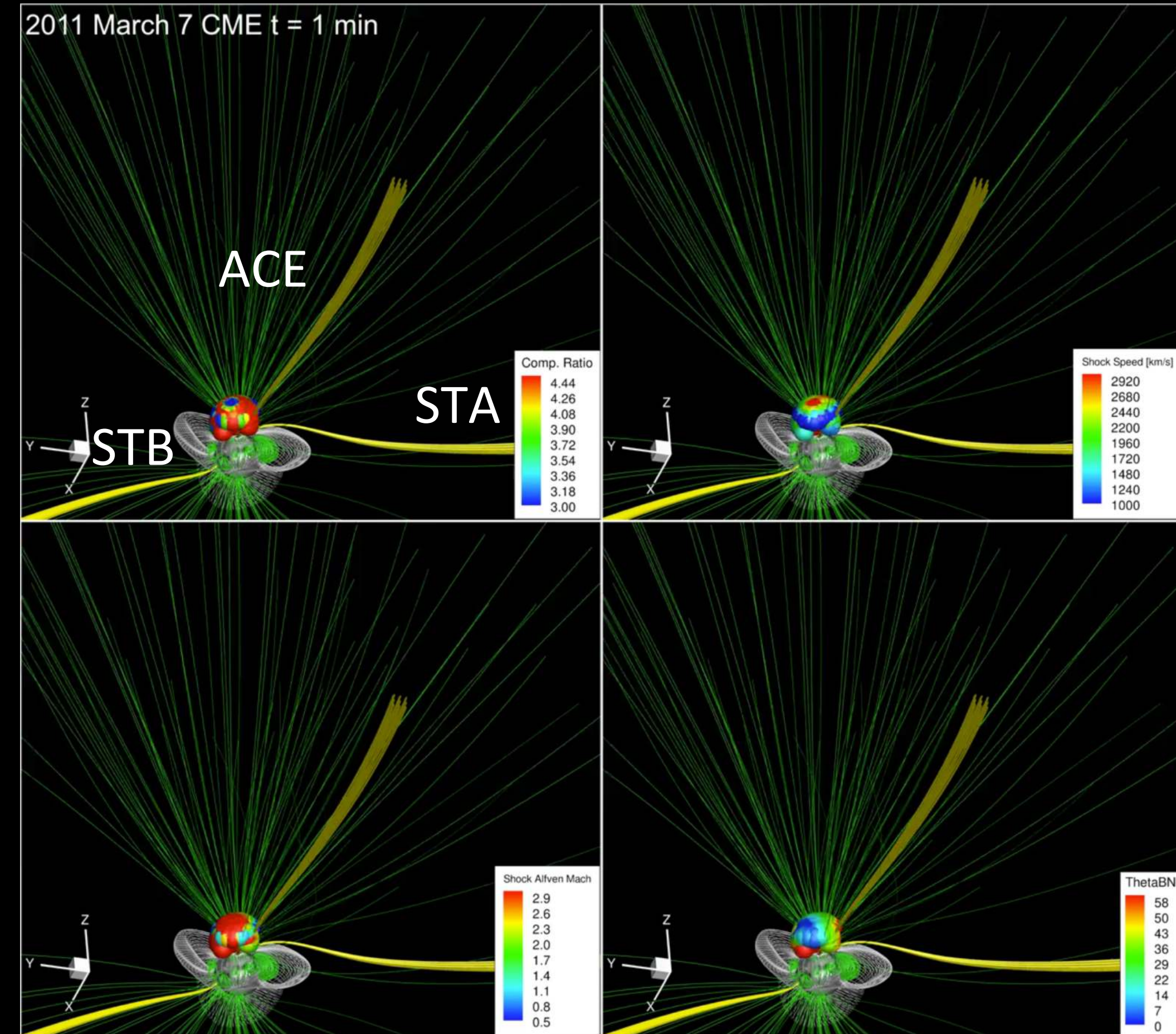
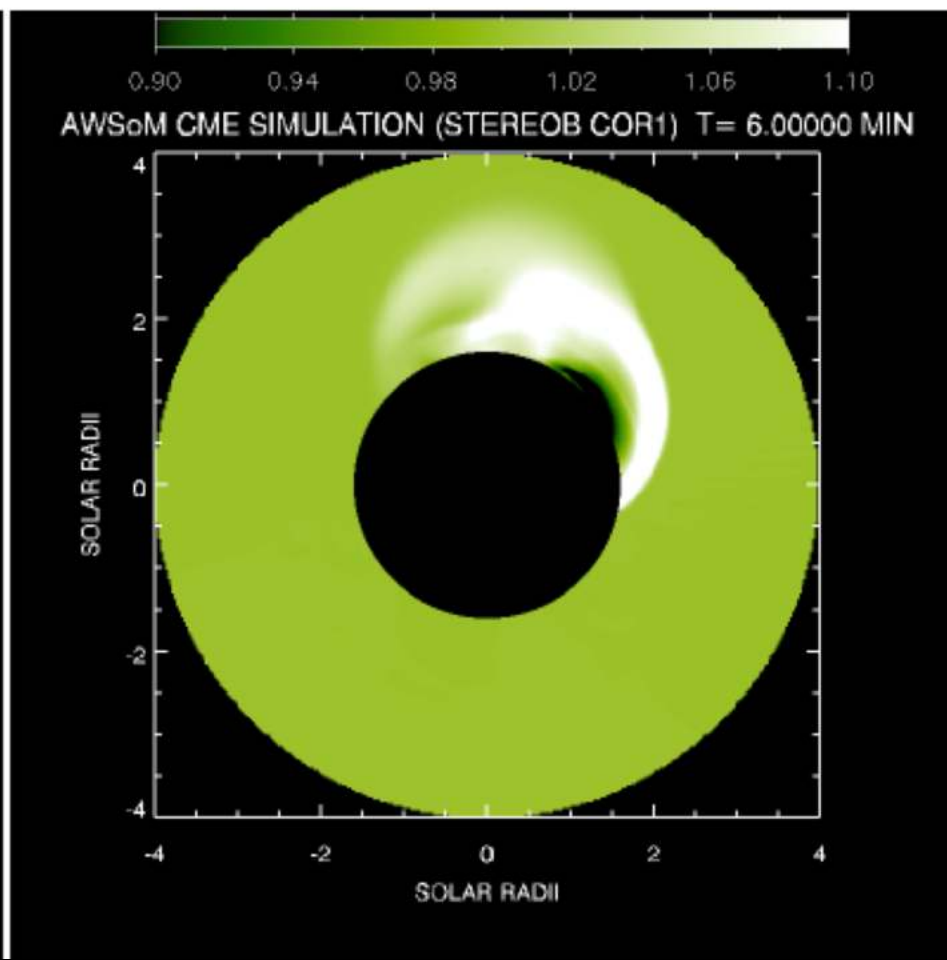
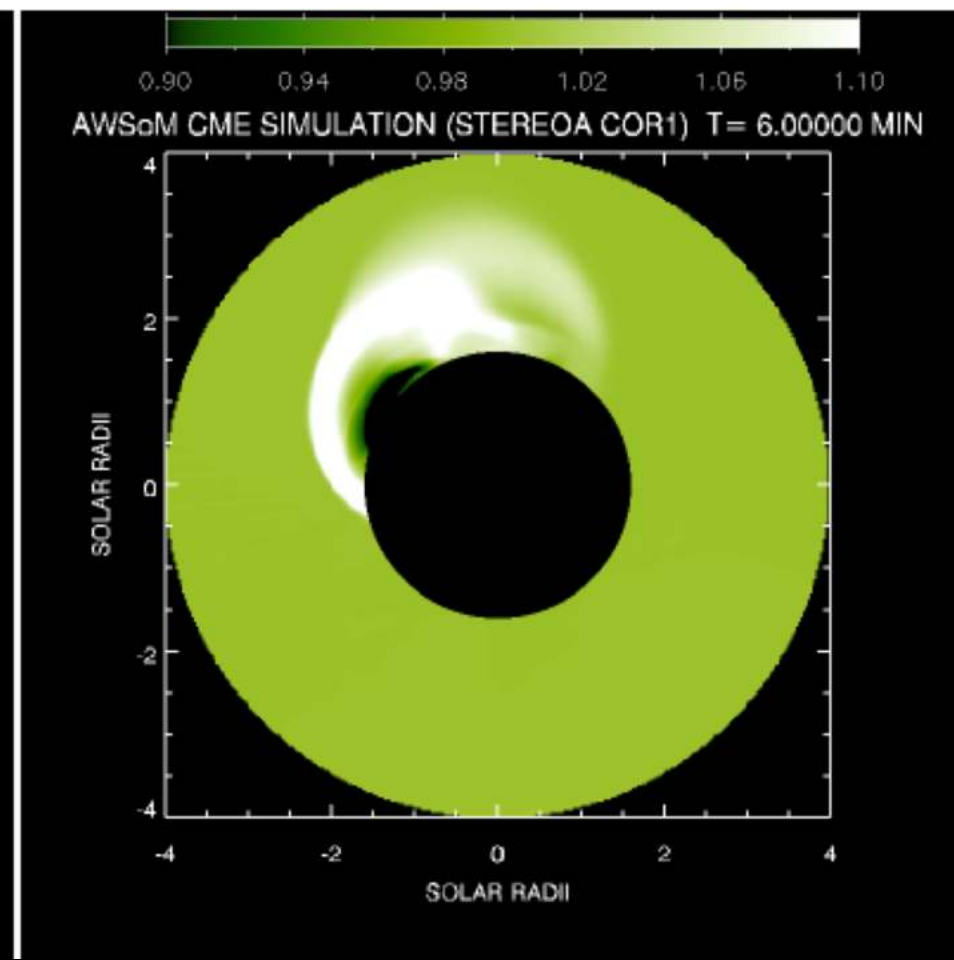
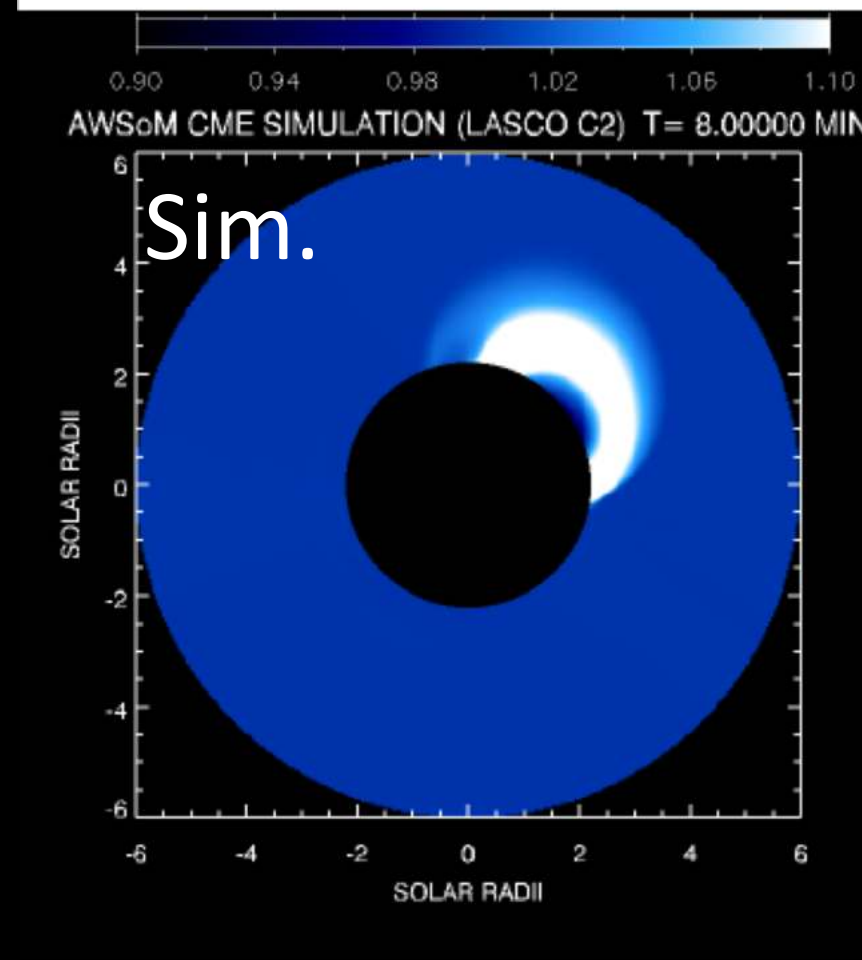
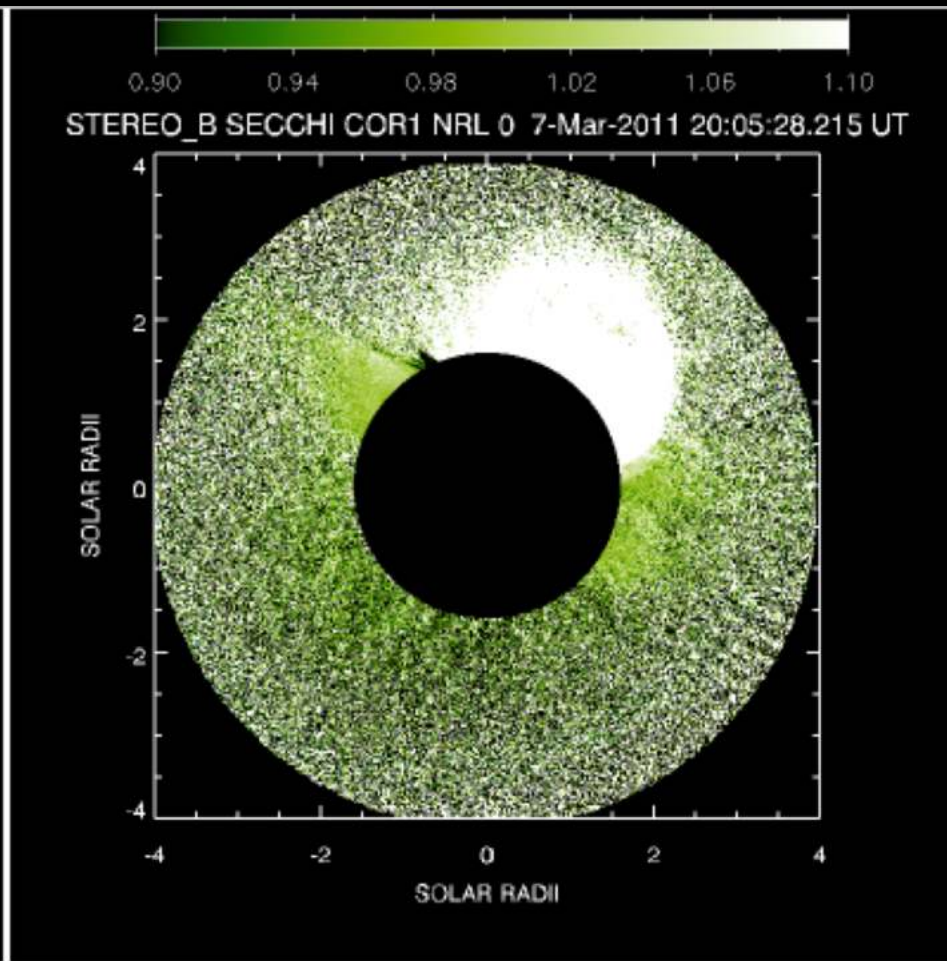
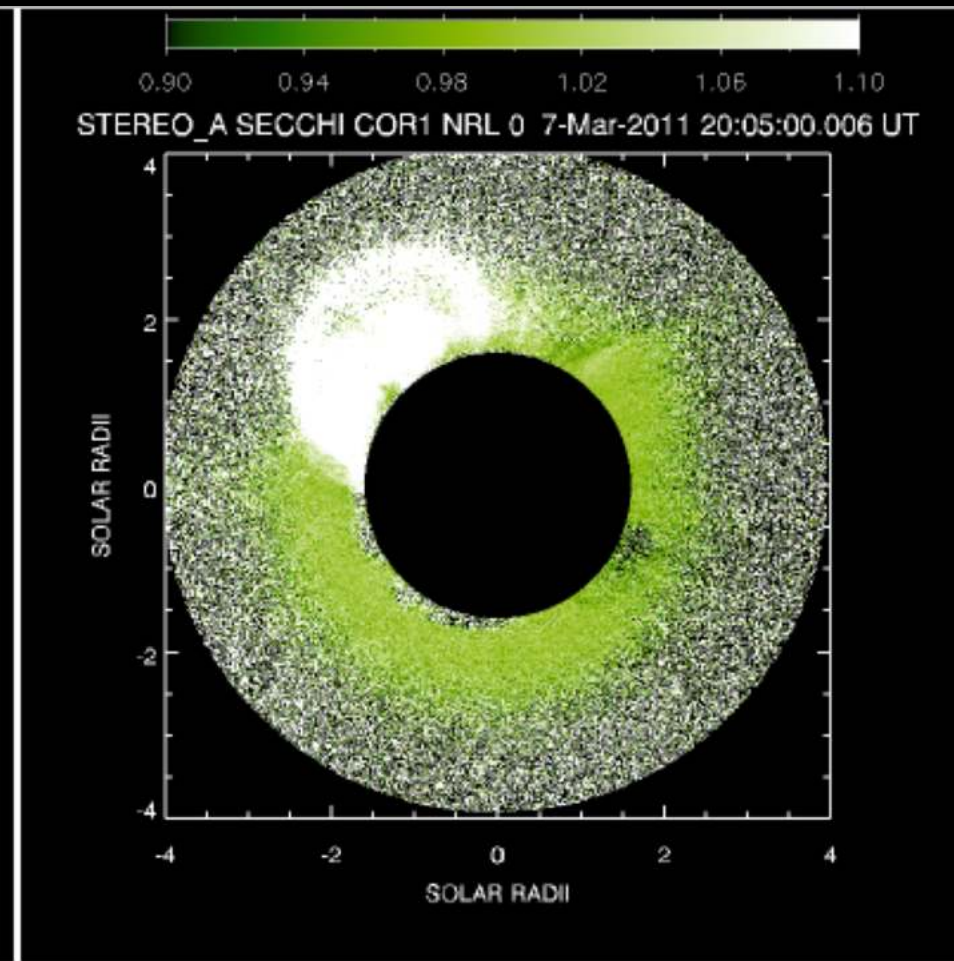
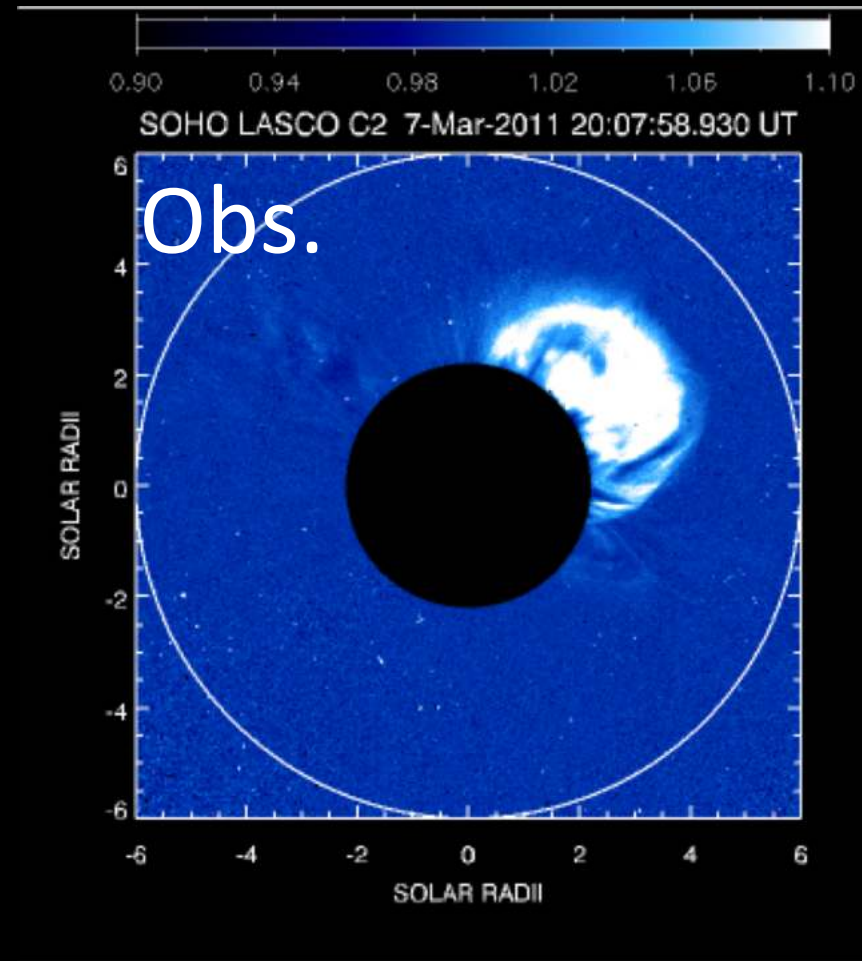
CME-driven Shocks (2011 March 7 Event)

LASCO C2

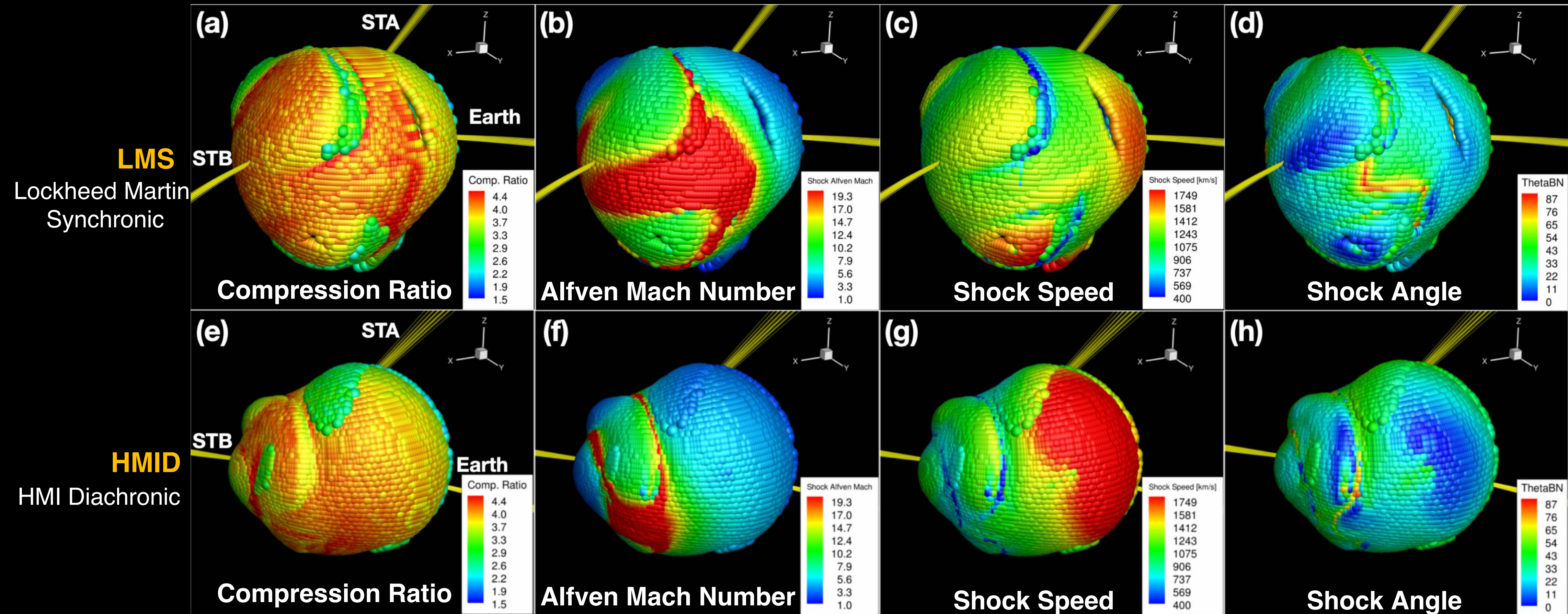
STA COR1

STB COR1

Shock Evolution in the Simulation



Influence of Background Corona on the CME-driven Shock

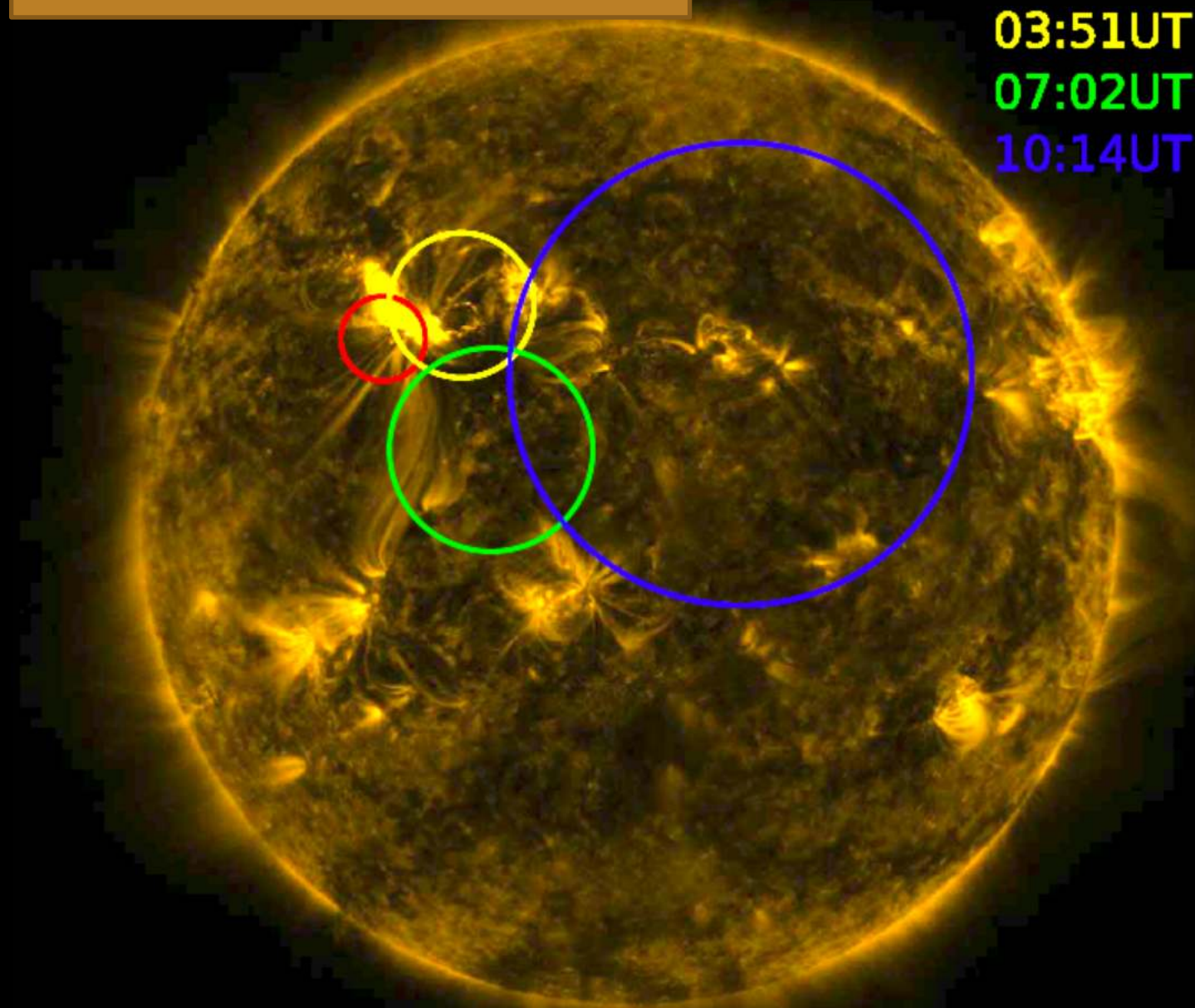


Jin et al. 2022b

- The ambient corona and solar wind have a big impact on the CME-driven shock parameters, therefore the particle acceleration process involved as well as the SEP observed in-situ.
- In addition to improve the magnetic input of the model, **better constrains of the plasma environment of the CME source region is critical, especially to correctly capture the early phase shock evolution.**

MUSE Science: Link to CME-shock & Particle Acceleration

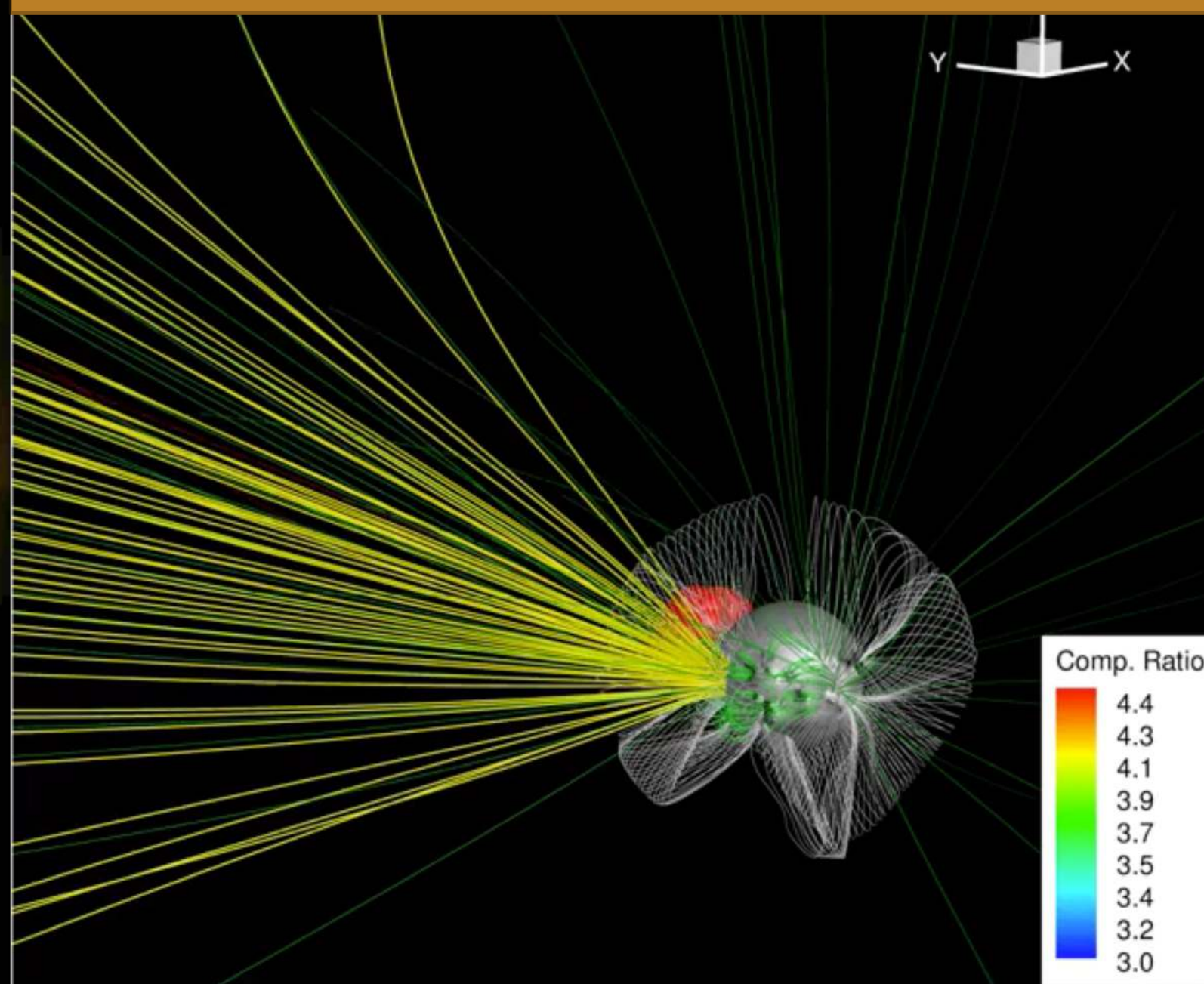
2012 March 7 Event



Emission Centroid Migration

00:40UT
03:51UT
07:02UT
10:14UT

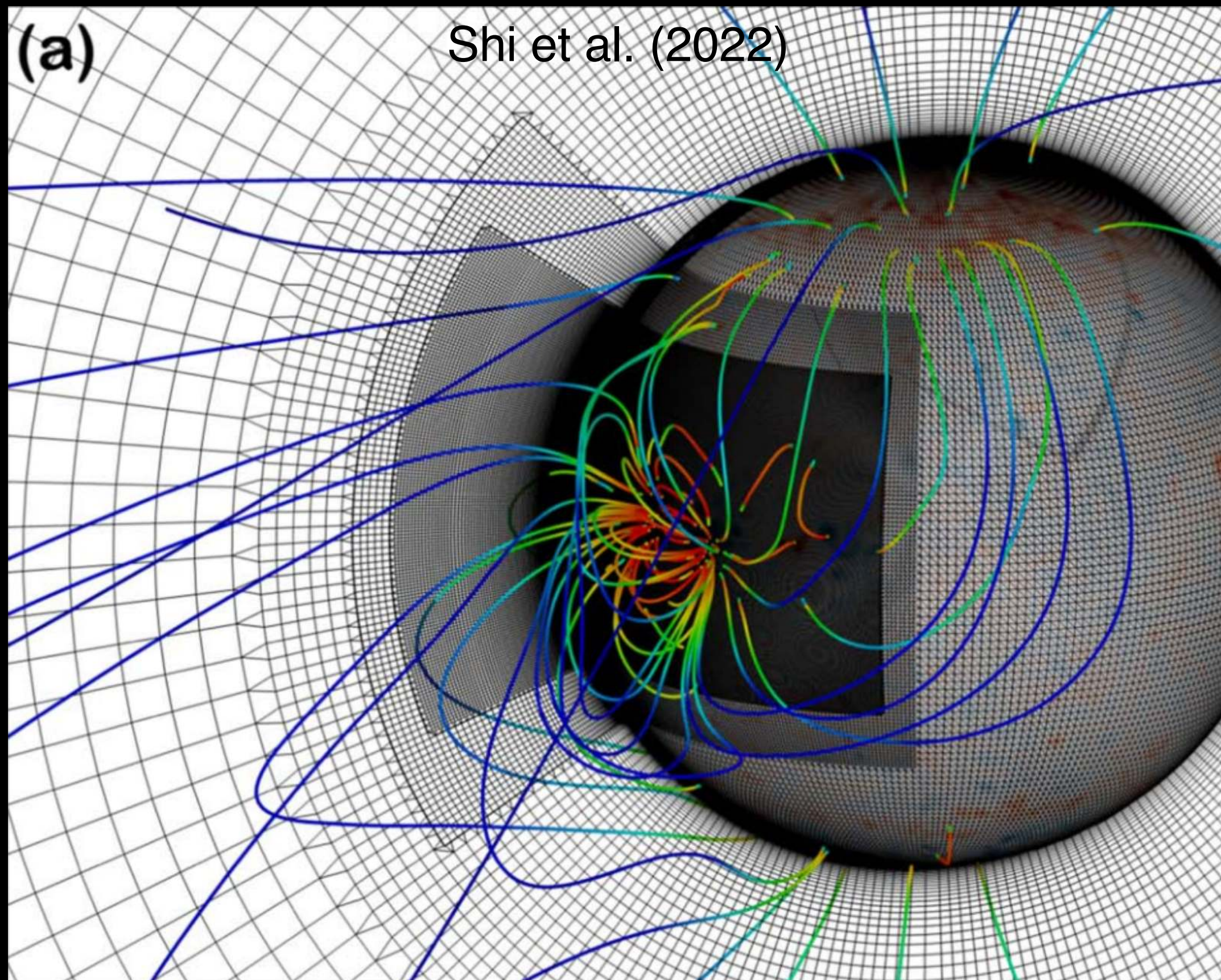
2014 September 1 BTL Event Simulation



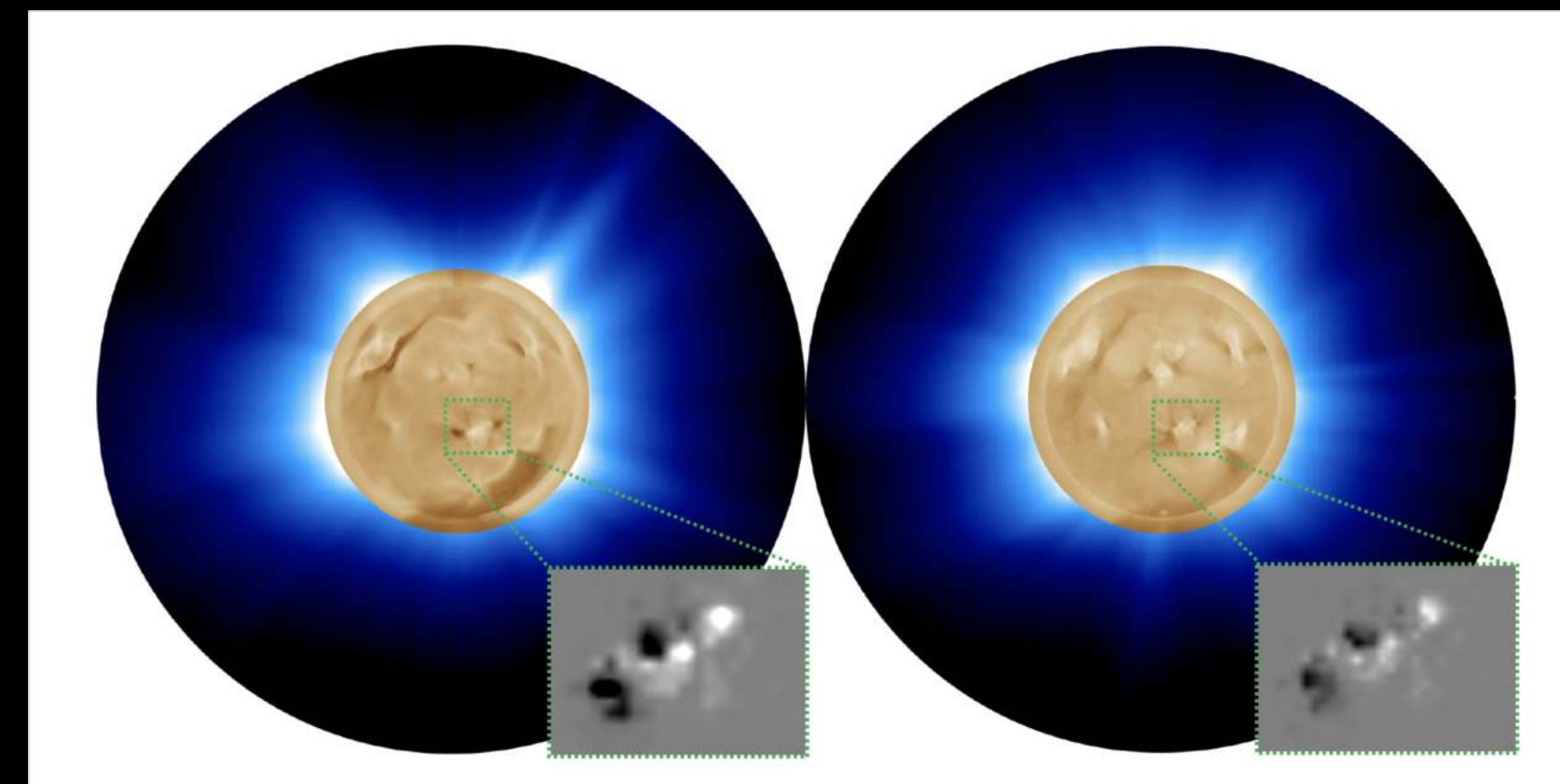
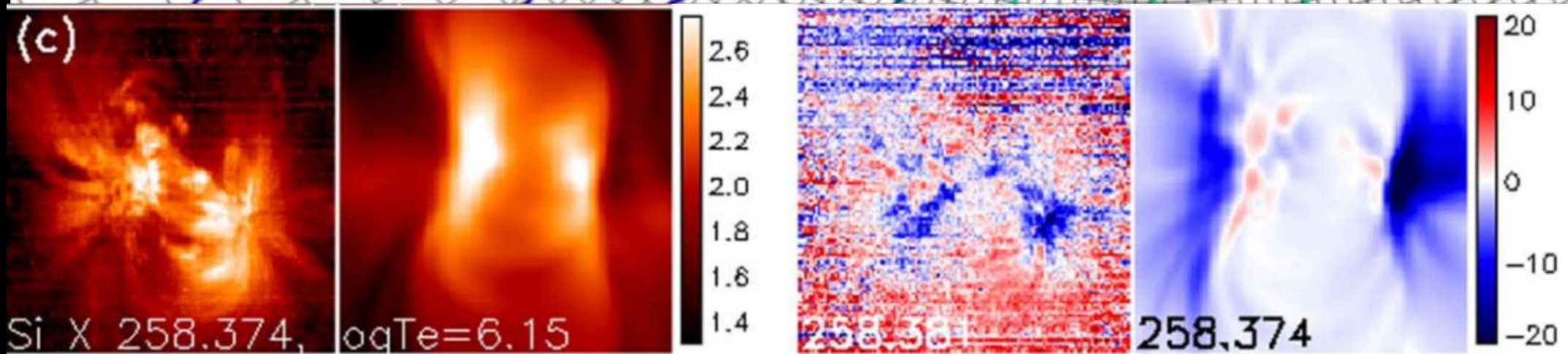
The uniqueness of MUSE is the possibility of observing the low-corona footprints of the shock flank (Veronig et al. 2011, Harra et al. 2011) and the footpoints of the gamma-ray emission region, therefore providing critical information for the source/mechanism of particle acceleration.

- **Fermi** has observed three **Behind-the-limb** gamma-ray flares and flares with **moving gamma-ray centroids**, which pose a puzzle and challenge on the particle acceleration and transport mechanisms.
- Recent modeling (Plotnikov et al. 2017, Jin et al. 2018) and observations (Gopalswamy et al. 2018, Kahler et al. 2018) suggest CME-driven shock may play an important role. However, there is still a hot debate (Hutchinson et al. 2020) on whether these particles are accelerated by the shock, the solar flare, or both.

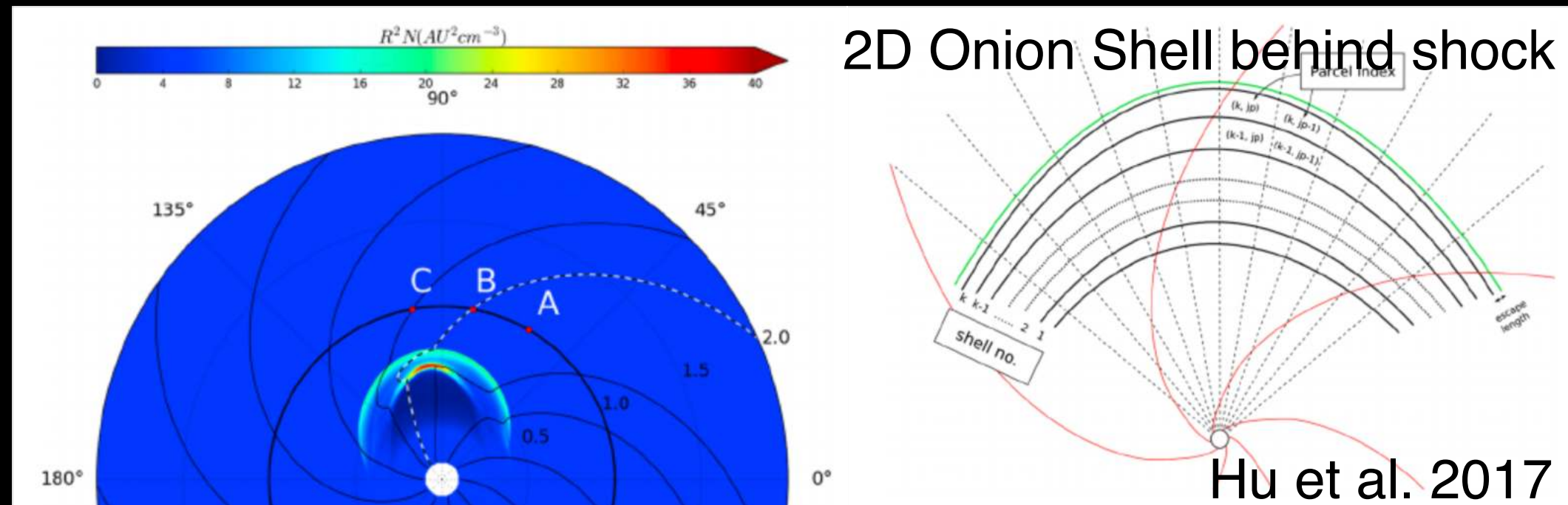
Future Model Improvement



- Improve the model resolution of active region by **adaptive mesh refinement**, together with **high-order scheme** to resolve finer corona structures.
- Improve the **input magnetic map** (e.g., higher resolution), ensembled modeling to evaluate **uncertainty of the far-side/polar field**.
- Improve on CME initiation model:
 - Improve **EEGGL** module by specifying early velocity profile of the flux rope that will be observed by MUSE.
 - Equilibrium flux rope insertion (Titov et al. 2014, Sokolov 2022).
- Couple with **particle acceleration and transport code** for modeling not only the **SEPs** to 1AU but also energetic particles tracing back to the surface of the Sun.



iPATH Model



- **iPATH** model numerically solves particle acceleration at a propagating shock and subsequent transport of these particles in the solar wind.
- **2D onion shell** module tracking SEPs downstream of the shock.
- Particles escaping upstream are followed using a Monte-Carlo approach, where both **along-field** and **cross-field** diffusion are included.
- **Revising the 2D parcel structures to 3D cell structure using AWSoM MHD shock and plasma inputs.**

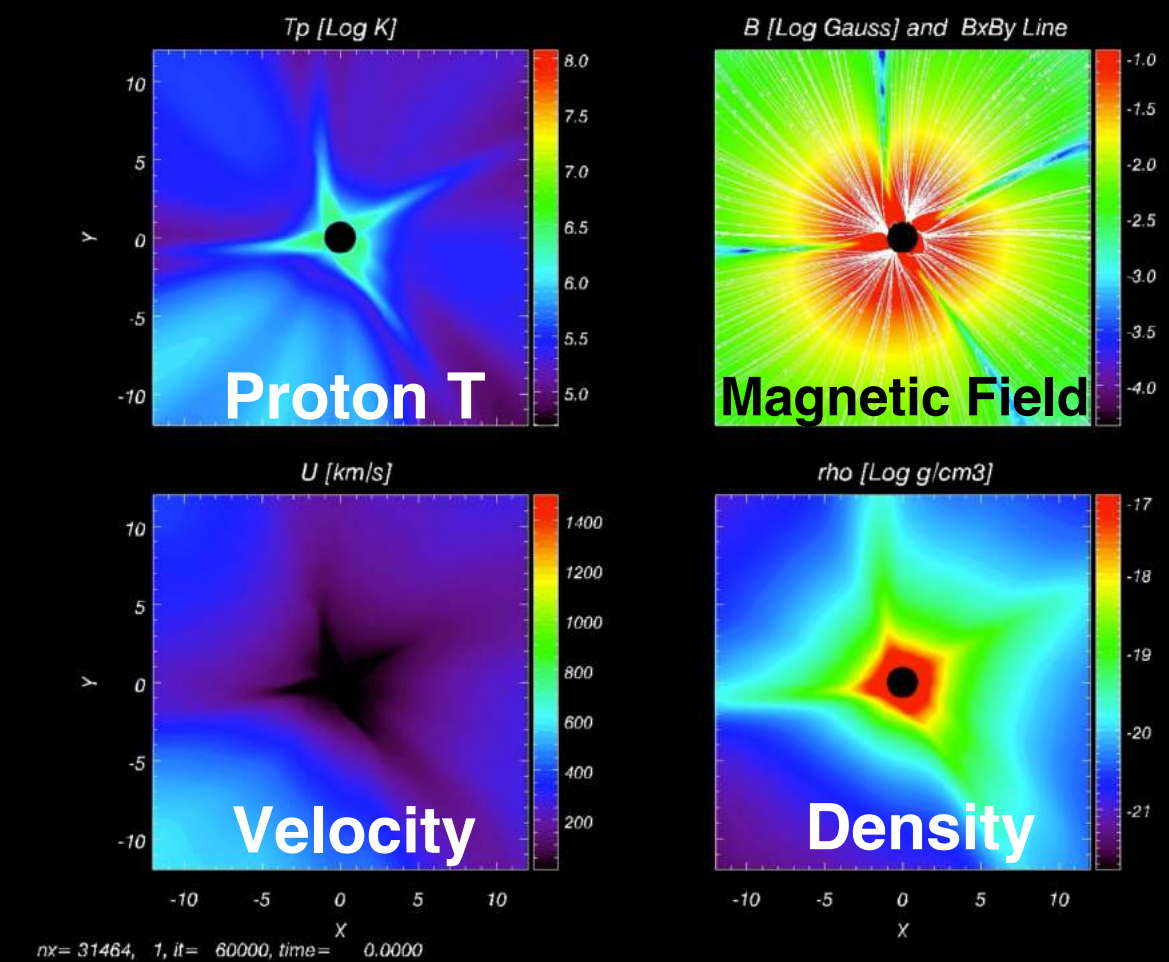
Shock Location

Shock Parameters

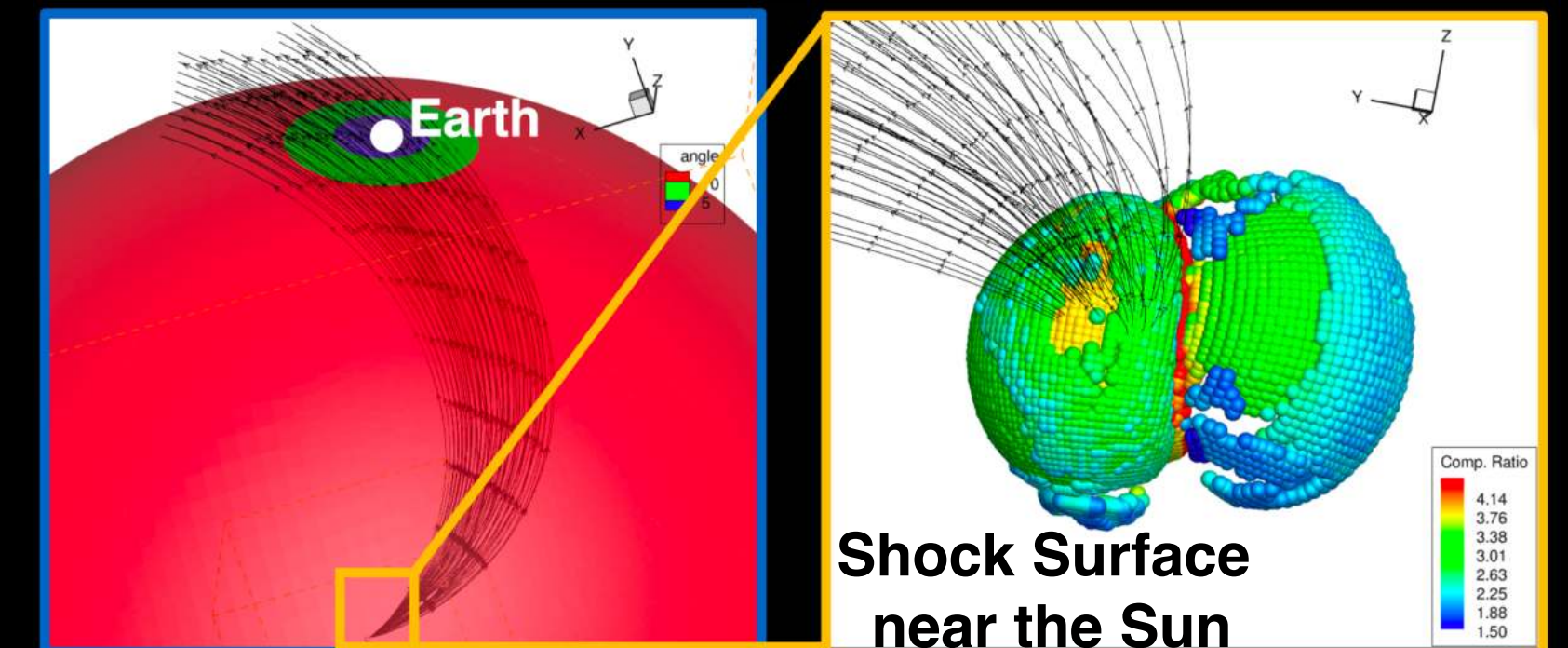
Shell Location

Downstream Plasma

AWSoM MHD



Ensemble Modeling



- Trace **65** field lines within **10** degree of Earth location at **1 AU**.
- The angular spread is also supported by the **cross field diffusion** studies.

Thank you!

